African Journal of Biotechnology

Volume 16 Number 28, 12 July, 2017

ISSN 1684-5315

Academic Journals

ABOUT AJB

The African Journal of Biotechnology (AJB) (ISSN 1684-5315) is published weekly (one volume per year) by Academic Journals.

African Journal of Biotechnology (AJB), a new broad-based journal, is an open access journal that was founded on two key tenets: To publish the most exciting research in all areas of applied biochemistry, industrial microbiology, molecular biology, genomics and proteomics, food and agricultural technologies, and metabolic engineering. Secondly, to provide the most rapid turn-around time possible for reviewing and publishing, and to disseminate the articles freely for teaching and reference purposes. All articles published in AJB are peer-reviewed.

Contact Us

Editorial Office: ajb@academicjournals.org

Help Desk: helpdesk@academicjournals.org

Website: http://www.academicjournals.org/journal/AJB

Submit manuscript online http://ms.academicjournals.me/

African Journal of Biotechnology

Table of Content: Volume 16 Number 28 12 July, 2017

ARTICLES

academicJournals

Vol. 16(28), pp. 1561-1566, 12 July, 2017
DOI: 10.5897/AJB2016.15378
Article Number: 32B9D5D65092
ISSN 1684-5315

http://www.academicjournals.org/AJB

African Journal of Biotechnology

Full Length Research Paper

Effect of resin from *Commiphora swynnertonii* on white blood cell and selected haematopoietic organs in albino mice (*Mus musculus*)

Bakari G. G.[1]*, Ceaser G.[2], Max R. A.[1] and Mbasa G. K.[1]

[1]Faculty of Veterinary Medicine, Sokoine University of Agriculture, P. O. Box 3017, Morogoro, Tanzania.
[2]IITA, Dar es Salaam, Tanzania.

Received 1 April, 2016; Accepted 24 October, 2016

Commiphora swynnertonii **is among the most commonly used medicinal plants by pastoralist communities especially in northern regions of Tanzania. The effect of resin from this plant on white blood cells (WBC) and haematopoietic organs was studied using albino mice. Sixty adult mice were randomly assigned into four groups (n = 15). G1 acted as control whereas G2, G3 and G4 received oral doses of 50, 100 and 200 mg resin per kg body weight, respectively for 35 days consecutively. Blood samples for differential and total WBC count were collected before treatment and on days 7, 14, 28 and 35 after treatment. Also, three mice from each group were humanely sacrificed before treatment, on day 14 and 35 after treatment. Sternum, liver and spleen samples from sacrificed mice were collected for assessment of any effects of the resin on haematopoietic organs. Results showed that mice in G2 and G4 had a significant increase (P < 0.05) in total WBC counts by day 7 as compared to the control group. This trend was then followed by a gradual decrease towards end of the experiment. No significant changes in total WBC counts were observed in G3 following treatment. The effect of *C. swynnertonii* resin on differential WBC count was non-specific and insignificant; G1 and G2 mice had their lymphocyte and monocyte counts slightly increasing with time while that of G3 and G4 decreased slightly or remained unchanged. Neutrophils counts decreased significantly in G1 and G2, but there were no significant changes for G3 and G4. Changes in the haematopoietic tissues following exposure to the resin included increased cellularity of sternal bone marrow as compared to spaces occupied by adipocytes. In particular, there were different developmental stages of granulocytes, erythroblasts and all megakaryocytic series. Small patches of erythropoietic series and lymphoblastic cells were observed in the liver and spleen respectively of the mice that received resin. It is concluded that oral administration of *C. swynnertonii* resin to mice caused a significant but transient increase in total white cell counts as a short-term effect. Prolonged exposure to the resin was associated with changes in the haematopoietic system such as increased cellularity of bone marrow and erythropoietic patches in liver and spleen.**

Key words: *Commiphora swynnertonii*, resin extract, WBC count, haematopoietic tissue, albino mice.

INTRODUCTION

The use of plants for treatment of various diseases affecting humans and animals is a common and popular practice in many developing countries (Idowu et al., 2009). *Commiphora swynnertonii*, a tropical shrub belonging to Burseraceae family and widely distributed in Africa, is among such plants. Different parts of the plant have been used by pastoralists for treatment of bacterial and fungal infections (e.g., tuberculosis, abscesses,

dysentery, gastrointestinal ulcers, wounds, ringworms and candidiosis), control of ecto- and endo-parasites (Kaoneka et al., 2007), and rheumatism (Minja, 1999). Studies by Bakari et al. (2012, 2013) demonstrated that resin extracts from *C. swynnertonii* had significant biological activities against Newcastle virus, bacteria (*Staphylococcus aureus, Escherichia coli* and *Pseudomonas aeruginosa*) fungi (*Candida albicans* and *Actinomyces pyogenes*), and protozoa (*Coccidia* spp.) using *in- vitro* and *vivo* test systems. It was further observed that the *C. swynnertonii* resin affected some hematological and biochemical parameters during *in vivo* trials using chickens, guinea pigs and rabbits. For instance, Bakari et al. (2015) found that oral administration of the resin extract was associated with an increase in white blood cell (WBC) counts, particularly monocytes and lymphocytes, in growing chickens, that is, immuno-potentiating effect. This observation is interesting because drugs or supplements with immuno-potentiating effects are vital in patients or individuals with immune-compromising conditions such as acquired immune disease syndrome (AIDS), tuberculosis (TB), cancers and many others. Extracts from other medicinal plants such as *Commiphora mukul* and *Commiphora molmol* have been reported to increase the WBC count in mice (Abdallah et al., 2009; El-Naggar, 2011). The effect of *C. swynnertonii* resin extracts on the immune system in animals has not yet been reported.

The current study was therefore designed to investigate the effect of oral administration of *C. swynnertonii* resin on peripheral white blood cell counts and major haematopoietic organs (bone marrow, spleen and liver) in chickens.

MATERIALS AND METHODS

Source of test resin and preparation

C. swynnertonii resin was collected from the northern Tanzania District of Simanjiro in Manyara Region located at 4°0′0″ S, 36°30′0″ E; 1,360 m above sea level. To harvest the resin, a thin band of bark was removed near the base of the tree and an incision was made at a depth of about half the thickness of the bark to allow resin to ooze from the cortex and was collected in an airtight container. Preparations involved soaking of the resin in 99.8% ethanol followed by separation using a rotary evaporator. The resulting crude extracts were then stored at 4°C in air-tight bottles until used in this experiment.

Experimental design and resin administration

Forty albino mice aged between 2 and 3 weeks old and ranging between 100 and 130 g were divided into four groups (n = 15) and were caged separately. The mice were maintained on broiler mash as basal feed with *ad libitum* drinking water. The resin was diluted in distilled water to make a stock solution of 50 mg per mL. The control group (G1), received an oral placebo (distilled water). The remaining groups (G2 - G4) received varying oral doses of resin using a 5 mL graded syringe as shown in Table 1. The resin was administered for 35 consecutive days. Before and after treatment with resin, all mice in all groups were closely monitored throughout the experiment for any sign of toxicity that could be associated with the resin.

Table 1. Grouping and treatment allocation.

Group (n = 15)	Amount of resin administered (mg/kg body weight)
G1 (Control)	0 (distilled water)
G2	50
G3	100
G4	200

Sampling and preparation

Determination of white blood cells counts

Three mice from each group were humanely sacrificed, on days 0, 7, 14, 21 and 35, by placing the mice in an induction chamber containing chloroform-soaked cotton wool until they were fully anaesthetized. Then, blood samples were obtained through heart-puncture using EDTA vacutainer tubes. The blood samples were used to prepare thin blood smears for total white blood cells (WBC) counts. For determination of differential WBC counts, blood was diluted using glacial acetic acid at a ratio of 1:20 and then counted using Neubauer chamber.

Assessment of haematopoietic organs

Spleen, liver and bones from sternum and femoral epiphysis of three mice from each group sacrificed on days 0, 14 and 35 were collected and fixed in formaldehyde. The spleen and liver were processed and stained with hematoxyline and eosin (H&E) for histological examination. The bones were decalcified in formic acid to expose the bone marrow before squash smears were made and stained using Giemsa method for examination of haematopoietic cells. Haematopoiesis was assessed quantitatively by examining density of cellularity and mitosis in the histological sections. Bone marrow was assessed by evaluating/comparing haematopoietic and adipocytes areas as follows: + means that 50% of the haematopoietic area is covered by haematopoietic cells and 50% by adipocytes; ++ means that 60% of the haematopoietic area is covered by haematopoietic cells, 40% adipocytes; +++ means that greater than 70% of the haematopoietic area is covered by haematopoietic cells and a small area is covered by adipocytes.

Statistical analysis

The data were subjected to ANOVA using Microsoft Excel 2007.

*Corresponding author. E-mail: manemgay@yahoo.com.

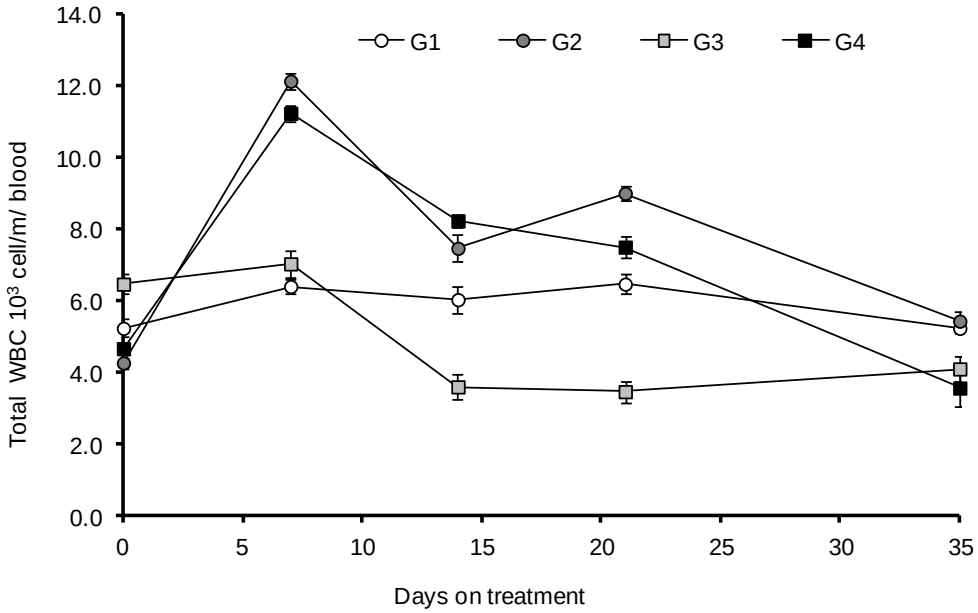

Figure 1. Total white blood cell counts following oral administration of varying doses of resin from *C. swynnertonii.*

The Student's t-test (at 95% confidence interval and significance level of 5%) was used to compare the effect of different resin doses among treatment groups. Mean differences with $P \leq 0.05$ were considered to be significantly different.

RESULTS

Behavioral changes

This study aimed at determining the effect of resin from *C. swynnertonii* on white blood cell count (immune system) and haematopoietic organs in mice. Neither behavioral changes nor signs of toxicity were observed following the oral administration of resin.

White blood cell counts

Total white blood cell counts of mice following oral administration of the resin are presented in Figure 1. An increase in total WBC count was only observed in G2 and G4 and it was only significant ($P<0.05$) on day 7 post-treatment. On the other hand, the levels in G3 remained below that of control group and by the end of experiment, there was no significant difference among the four groups. This suggests that the resin had a positive but only a transient effect on the number of WBC in the mice.

Differential WBC counts are presented in Table 2. Results indicated that administration of CS resin did not cause any significant changes in differential WBC counts and did not reflect the treatment. Comparison of either total or differential WBC counts between control and resin-treated groups at the end of experiment (on day 35) revealed no significant differences.

Haematopoietic organs

Bone marrow

Before the oral administration of resin, haematopoietic cell stimulation was very low and the bone marrow was not active in all the groups. At this stage, bone marrow was occupied by 50% of the adipocytes and less that 50% of haematopoietic cells (Figure 2A). Following administration of the resin, cellularity in the bone marrow increased in a dose-dependent manner with doses not exceeding 100 mg resin per kg body weight (Figure 2B and C). At the lowest dose of 50 mg (G2), more than 60% was covered by haematopoietic cells and the remaining area was covered by adipocytes. In the group that received 100 mg/kg (G3), the bone marrow was very active and the general cellularity was far above 70% with metamyelocytes, megakaryocytic and granulocytic cells being clearly visible in the histological sections. Bone marrow sections from G4 had more adipocytes vacuoles than those in G2 and G3. Figures 2A to C demonstrates the dose-dependent changes in cellularity of sternal bone marrow tissue sampled on day 35 of the experiment.

Liver and spleen

The effect of the resin on haematopoietic activity of the liver had a very similar trend with that of the bone

Table 2. Differential WBC count following oral administration with various doses of resin from *C. swynnertonii.*

Group	Cell type	Days on treatment				
		0	7	14	21	35
G1	Lymphocytes	54.0±2.3	57.9 ± 2.3	65.7±4.5	62.9±4.6	67.7±6.7
(0mg/kg)	Monocytes	1.6±0.2	3.6±0.3	3.2±0.7	1.0±0.4	2.4±0.6
	Neutrophils	43.8±2.0	37.6±1.6	30.8±4.2	37.5±2.2	29.2±2.2
G2	Lymphocytes	49.5±0.3	64.0±3.2	70.7±3.7	67.4±2.6	70.5±1.9
(50mg/kg)	Monocytes	2.4±0.2	5.1±0.8	2.6±0.4	2.4±0.5	3.4±0.4
	Neutrophils	47.7±1.4	37.7±3	27.3±3.9	30.7±4.1	26.8±2.8
G3	Lymphocytes	40.3±0.6	33.3±2.8	36.2±4.1	35.2±6.7	31.7±4.2
(100mg/kg)	Monocytes	0.7±0.1	3.3±0.1	3.0±0.6	2.5±0.4	2.5±0.5
	Neutrophils	30.3±1.4	33.8±0.4	27.8±5.2	30.3±4.7	32.1±2.1
G4	Lymphocytes	62.7±1.4	66.2±4	62.6±4.5	59.5±2.5	62.0±1.6
(200mg/kg)	Monocytes	0.6±0.2	1.6±0.4	2.4±0.4	0.6±0.2	2.1±0.3
	Neutrophils	34.5±0.9	28.4±1.9	35.1±4.2	40.4±1.4	36.3±3.3

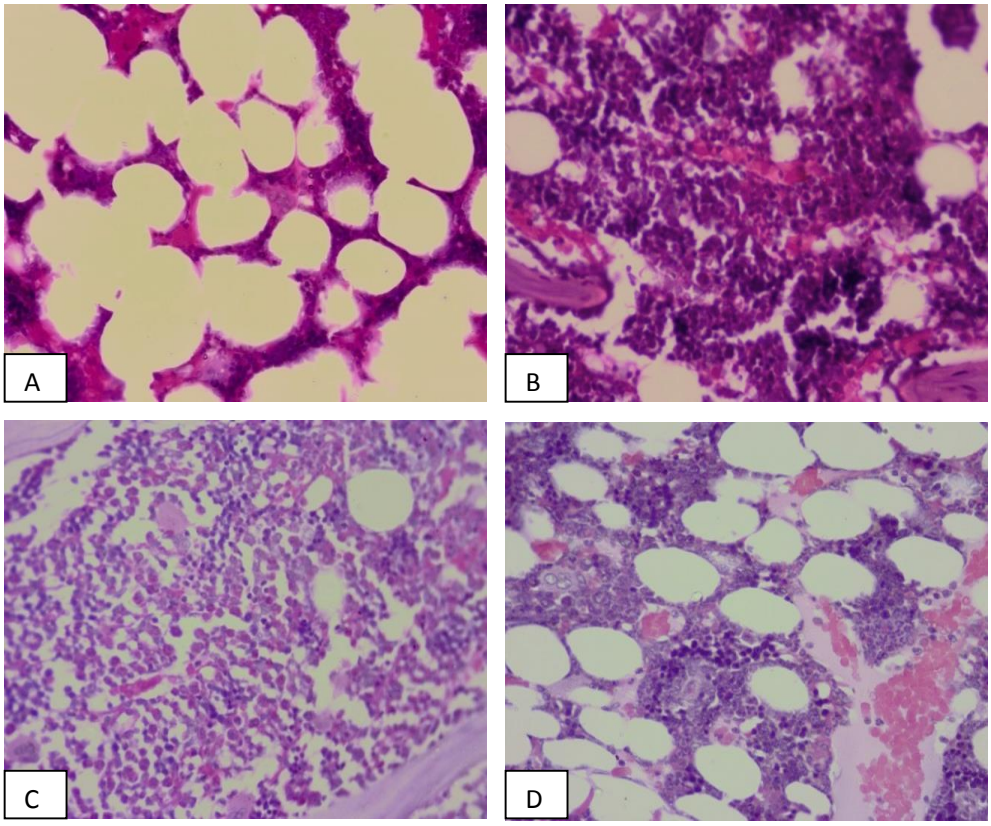

Figure 2. Bone marrow tissue sections (x40) taken on day 35 of the experiment. [A] Control group before administration of resin; [B and C] G2 and G3 with more haematopoietic cells than adipocytes; [D] more adipocytes than haematopoietic cells.

marrow. Prior to the administration of the resin, liver sections showed normal hepatocytes with no evidence of haematopoietic activity (Figure 3A). Administration of the resin induced haematopoiesis as evidenced by presence of dividing polychromatophilic cells (Figure 3B). This tendency was more pronounced in G3 mice, which

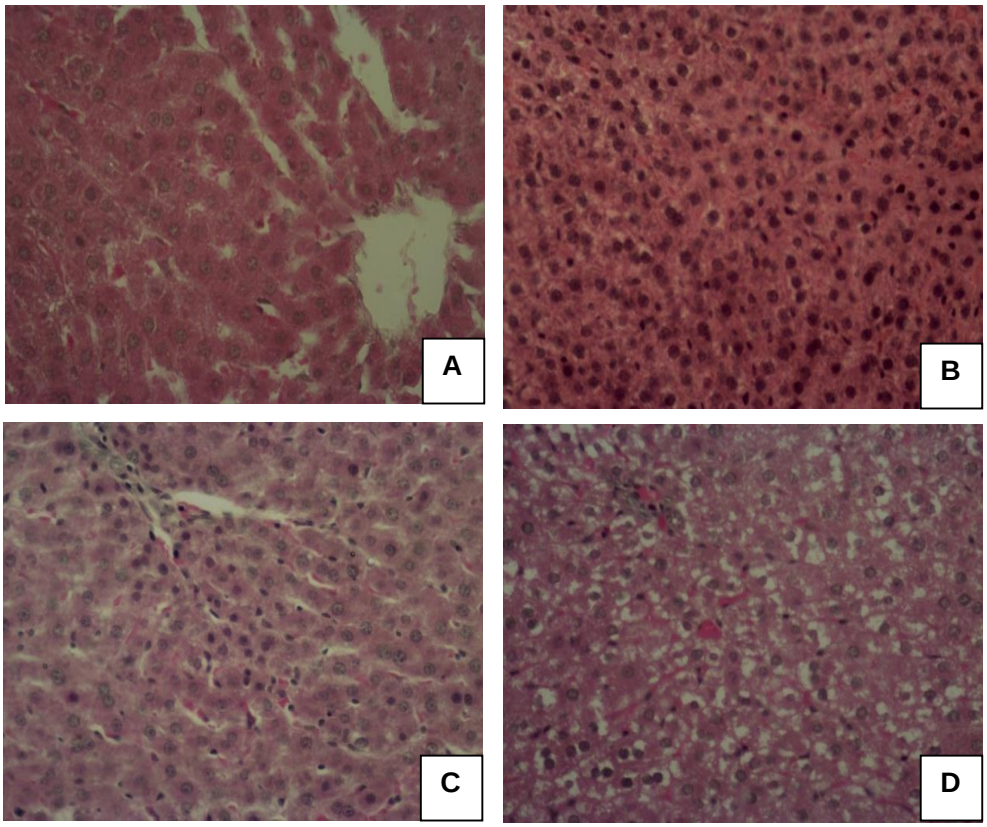

Figure 3. Liver tissue sections (x 40) taken on day 35 of the experiment. [A] Liver section from control group before administration of resin from *C. swynnertonii* [B and C] liver section from G2 and G3 with more dividing polychromatophilic cells; [D] liver tissue showing degeneration of hepatocytes was observed as whitish patches between cells.

received 100 mg/kg. However, in mice treated with 200 mg/kg (G4), degeneration of hepatocytes was observed as whitish patches between cells (Figure 3D). In the spleen, increased numbers of lymphoblastic cells were observed as compared to those not treated with resin.

DISCUSSION

This study aimed at determining the effect of resin from *C. swynnertonii* on white blood cell count (immune system) and haematopoietic organs in mice. Absence of behavioral changes following the oral administration of varying doses of resin to mice was an indication that the tested doses were mild and well tolerated by the animals. Signs of toxicity including general body weakness and diarrhea were observed in mice that received oral doses higher that 200 mg/kg body weight of *C. molmol* (Abdallah et al., 2009).

Leukocytes (WBC) proliferation has been used as reliable indicator to make variety of clinical decisions for both the appropriateness of treatment and for surgical intervention. Also, WBCs are major cellular component of the immune system and hence their response to proliferate is critical factor in evaluating the effectiveness of the immune system response. The current study has observed a significant but only a transient increase in total WBC counts following administration of the resin. Furthermore, the changes in WBC counts were not dose dependant. These findings are somehow contrary to those reported in similar studies using other *Commiphora* spp. Abdallah et al. (2009) found no significant increase in the WBC numbers following administration of *C. molmol* oleo-gum resins in rat, whereas El-Naggar (2011) observed a significant increase in WBC counts in rats treated with myrrh from *C. molmol*. Studies by Haffor (2010) revealed that *C. molmol* activated proliferation and differentiation pathway for all types of leukocytes during effective phase of specific immune responses. Significantly increased total WBC counts were reported in chickens that received higher dose of *C. swynnertonii* (Bakari et al., 2013), suggesting that low dosage used in the current study could be the reason behind the contrasting results.

Decreased WBC count following administration of high doses of *Commiphora* extract has also been reported

(Akinnuga et al., 2011; Ajali, 2004). This tendency has been associated with saponins, which are predominant bioactive constituents found in resin extract. Saponins are steroids or triterpenoid glycosides, common in a large number of plant products. They are glycosides with distinctive foaming characteristics and are natural detergents found in certain plants (Ajali, 2004). Saponins consist of a sugar moiety usually containing glucose, galactose, glucoronic acid, xylose, rhamnose or methylpentose, glycosidically linked to a hydrophobic aglycone (sapogenin) which may be triterpenoid or steroid in nature (Bachram et al., 2006; Unakalamba et al., 2013). A study done by Akinnuga et al. (2011) reported similar findings but for different plant species, *Gongronema latifolium,* that the presence of saponin in leaf extract of the plant significantly reduced all blood cells by suppressing the haematopoiesis system.

Despite the insignificant increase in WBC counts amongst groups, histological examination of bone marrow, liver and spleen from mice in this study revealed changes consistent with stimulation of haematopoietic system. Resin-treated mice had higher numbers of myeloblasts, myelocytes and metamyelocytes of granulocytes, erythropoietic and megakaryocytic series as well as lymphoblastic cells in the spleen. This suggests that prolonged exposure to resin beyond the current experimental period could greatly improve/potentiate the immune system.

It is concluded that oral administration of *Commiphora swynnertonii* resin to experimental mice transiently increased WBC counts and activated/stimulated the haematopoietic tissues. These findings imply that moderate levels of CS can be incorporated in animal feeds to improve cellular immunity.

Conflicts of Interests

The authors have not declared any conflict of interests.

ACKNOWLEDGEMENTS

The authors acknowledge the role of the Faculty of Veterinary Medicine, particularly the departments of Veterinary Physiology, Biochemistry, Pharmacology and Toxicology by guaranteeing laboratory facilitation and assuring ethical clearance.

REFERENCES

Abdallah EM, Khalid HE, Al-Khalifa SK (2009). Toxicological assessment of the oleo-gum resins of *Commiphora molmol* and *Boswellia papyrifera* in mice. J. Med. Plants Res. 3(6):526-532.

Ajali U (2004). Chemistry of Bio-compounds. First Edition. Rhyce Kerex Publishers, Enugu, Nigeria.

Akinnuga AM, Bamidele O, Ekechi P and Adeniyi OS (2011). Effects of an Ethanolic Leaf Extract of *Gongronema latifolium* on Haematological Some Parameters in Mice. Afric. J. Biomed. Res. 14:153 -156.

Bachram C, Sutherland M, Heisher I, Hebestreet P, Melzig MF, Fuchs H (2006). The saponin-mediated enhanced uptake of targeted saponin-based drugs in strongly dependent on the saponin structure. Exp. Biol. Med. 231:412-420.

Bakari GG, Max RA, Mdegela RH, Phiri EC, Mtambo MM (2012). Antiviral activity of crude extracts from *Commiphora swynnertonii* against Newcastle disease virus *in vivo*. J. Trop. Anim. Health Prod. 44(7):1389-93.

Bakari GG, Max RA, Phiri ECJ and Mtambo MMA (2013). Effect of resinous extract from Commiphora swynnertonii (Burrt) on experimental coccidial infection in chickens. Trop. Anim. Health Prod. 45 (2): 455-459.

Bakari GG, Max RA, Mdegela, RH, Pereka AE, Phiri ECJ and Mtambo MMA (2015). Effect of resinous extract from Commiphora swynnertonii (Burrt) on various physiological parameters in chickens. J. Medic.Plants Res. 9(13):462-470.

El-Naggar SA (2011). Lack of the Beneficial Effects of Mirazid (*Commiphora molmol*) When administered with Chemotherapeutic Agents on Ehrlich Ascetic Carcinoma Bearing Mice. Adv. Biol. Res. 5(4):193-199.

Haffor AS (2010). Effect of *Commiphora molmol* on leukocytes proliferation in relation to histological alterations before and during healing from injury. Saudi J. Biol. Sci. 17(2):139-146.

Idowu A, Taiwo Bola, Oboh O and Peniel N (2009). Properties of aqueous extracts of *Phyllasntus amarus* (Schum and Thonn) and *Xylopia aethiopica* (Dunal) in albino mice. Ethno-Med, 3(2):99-103.

Kaoneka B, Mollel M and Lyatuu F (2007). Leaf essential oils composition and tick repellency activity of *Commiphora swynnertonii.* J. Biol. Res. 8:213-216.

Minja MMJ (1999). The Maasai wonder plants. Paper presented at the people and Plants training workshop held at Tropical Pesticide Research Institute, Arusha Tanzania 15-18th March 1999.

Unakalamba BC, Ozougwu JC and Ejere VC (2013). Preliminary evaluation of the haematological effects of *Picralima nitida* saponin extracts on *Rattus novergicus.* Intl. J. Bio. Biol. Sci. 2(2):28-32.

academicJournals

Vol. 16(28), pp. 1567-1578, 12 July, 2017
DOI: 10.5897/AJB2017.15943
Article Number: 7A68A4765094
ISSN 1684-5315

http://www.academicjournals.org/AJB

African Journal of Biotechnology

Full Length Research Paper

Characterization of cassava starch films plasticized with glycerol and strengthened with nanocellulose from green coconut fibers

Bruna Aparecida Souza Machado[1,3]*, João Henrique de Oliveira Reis[2], Lindaiá Santos Cruz[2], Ingrid Lessa Leal[1,2], Josiane Dantas Viana Barbosa[3], Joyce Batista Azevedo[3] and Janice Izabel Druzian[2]

[1]Department of Food and Biotechnology, University Center SENAI CIMATEC, Serviço Nacional de Aprendizagem Industrial, Avenue Orlando Gomes, 1845 - Piatã, Salvador - BA, 41650-010, Brazil.
[2]Graduate Program in Food Science, Faculty of Pharmacy, Universidade Federal da Bahia, Barão de Jeremoabo Street, Ondina, Salvador - BA, 40170-110, Brazil.
[3]Health Institute of Technology, University Center SENAI CIMATEC, Serviço Nacional de Aprendizagem Industrial, Avenue Orlando Gomes, 1845 - Piatã, Salvador - BA, 41650-010, Brazil.

Received 15 February, 2017; Accepted 22 June, 2017

The aim of this study was to obtain and characterize biodegradable films of cassava starch plasticized with glycerol and reinforced with nanocellulose from coconut fibers. The mechanical and physical-chemical properties of the nano-biocomposites films obtained were evaluated. The method used to investigate the viability of incorporating coconut nanocellulose in films was applied through a statistical design of the response surface of 17 formulations containing three independent variables (starch, glycerol and nanocellulose). The films were prepared through casting technique, and the effect of different concentrations of the ingredients in each formulation was investigated by monitoring the dependent variables. The green coconut fiber was composed of 32% cellulose, 38% lignin and 0.25% hemicellulose resulted in nanocellulose with a length (L)/diameter(D) value of 38.9±4.7 after the acid hydrolysis process (64% H_2SO_4; 50°C; 10-15 min). The incorporation of nanocellulose resulted in significant changes ($p<0.05$) in the barrier and mechanical properties. Additionally, there was a significant increase in the Young's modulus and in the tensile of the nano-biocomposites. Consequently, there was a decrease in the percentage of elongation. Thus, films formulated from cassava starch plasticized with glycerol could have significantly altered mechanical, technical and barrier properties due to the incorporation of coconut nanocellulose.

Key words: Biodegradable packaging, cellulose nanocrystals, nano-biocomposites, coconut fibers.

INTRODUCTION

In the last few years there has been a great interest in the development of green technologies around the world for products that have lower environmental impact. Green chemistry, as a whole, involves the development of chemical processes and products that generate a cleaner, healthier and sustainable environment (Silva et al., 2009). Thus, synthetic plastic materials have received much attention because of their non-biodegradability and

non-renewable sources (Zhong et al., 2012; Meneguin et al., 2017; Chaichi et al., 2017).

One solution found to improve the environmental impact of synthetic plastics was the development of biomaterials from renewable polymers that can substitute synthetic materials. Starches are polymers with a high potential to produce flexible films and are inexpensive, biodegradable and highly available from renewable sources. However, the primary challenge is to substitute conventional packages while maintaining the same efficacy, quality and shelf-life. These results can be obtained through the control of mechanical properties and permeability (Seligra et al., 2016; Henrique et al., 2007; Qazanfarzadeh and Kadivar, 2016; Montero et al., 2017).

Ligno-cellulosic fibers are excellent raw materials for polymer and composites chemistry, which can be verified by the high number of patents and products already being commercialized with these fibers (Kermit, 2010; Ortega and Baillie, 2011; Sohei et al., 2011; Kun, 2011). Cellulose present in ligno-cellulosic fibers is formed by amorphous regions appearing as imperfections on micro-fibrils and by crystalline regions. The cellulose fibrils can be cleaved transversally when hydrolyzed in an acid medium, resulting in small crystals. These highly crystalline particles are referred to as nanocellulose, micro-crystalline cellulose, cellulose cristalito, nanocrystals of cellulose, whiskers or cellulose nano-whiskers when the L/D ratio is lower than 200 (Costa et al., 2016; Niu et al., 2017; Sun et al., 2017).

In recent years, various research groups have reported new techniques for the formation of nanocellulose from different natural sources (Myllytie et al., 2010; Rosa et al., 2010; Silva et al., 2012; Costa et al., 2014; Machado et al., 2014; Rusmirović et al., 2017; Wang et al., 2017), and the incorporation of nanocellulose into polymeric materials. Nanocellulose crystals have numerous advantages compared with other nano-structured materials, such as ease of formation, low cost of raw materials, diverse characteristics, which are dependent on the source of the natural substrate, and more beneficial mechanical properties compared with carbon nano-tubes and inorganic nano-fibers (Strurcova et al., 2006; Panaitescu et al., 2015; Qin et al., 2016; Li et al., 2016; Liu et al., 2017).

This work evaluates the incorporation of the nanocrystals nanocellulose from green coconut fibers in polymeric films produced with cassava starch and plasticized with glycerol.

MATERIALS AND METHODS

The following materials were used for this study: cassava starch (donated by Cargill Agricola SA), glycerol (Synth), coconut fiber (composed of 38% lignin and 32% cellulose) provided by Embrapa Agroindustria Tropical (Fortaleza, CE, Brazil). In addition, reagents such as sodium hydroxide, sodium hypochlorite, sulfuric acid (98.08%), acetic acid (Vetec) and cellulose membrane (D9777 – 100 FTO) for dialysis were obtained from Sigma-Aldrich.

Extraction of cellulose from coconut fiber

The method used to extract cellulose was adapted from previously published method by Rosa et al. (2010), Samir et al. (2005) and Machado et al. (2014). The coconut fibers were oven-dried in circulation air at 35°C for 5 h, crushed to obtain a fine particulate and sifted using a 40-mesh sieve. The samples (30 g) were then washed with a solution of NaOH 2% (1.200 mL) for 4 h under constant agitation at 80°C. The resulting solution was filtered and washed in water to obtain the pulp. The washing process was repeated four times to completely remove the water-soluble materials. After washing the fibers, the pulp delignification process was performed by bleaching, using a mixture of 1.7% sodium hypochlorite (300 mL) and a buffer solution (300 mL). The resulting solution was constantly agitated at 80°C for 6 h. Then, the solution was filtered and oven-dried in circulation air at 25°C for 10 h to obtain the cellulose. Finally, the cellulose was pulverized in a mill (Cadense Ltda - Brazil).

Preparation of films strengthened with green coconut cellulose

The films were processed using a casting technique, which consisted of the preparation of a filmogenic solution by dissolving the cassava starch in distilled water (3 to 6 g/100 g) and using glycerol as a plasticizer agent (0.5 to 2.5 g/100 g). Thereafter, a dispersion of nanocellulose (0.1 to 0.5 g/100 g) was added, which was previously heated to the starch's gelatinization temperature (70°C) under constant manual agitation. To prepare the filmogenic solution with approximately (40 g in mass), polystyrene Petri dishes were used. They were then dehydrated in a kiln with air circulation (35±2°C - Temperature range was used to avoid melting the petri dish and burning the film-forming solution) for 18 to 20 h (time required for complete drying). The obtained films were stored (60% relative humidity, 25°C) in a desiccator with a saturated sodium chloride solution for 10 days before being characterized (Veiga-Santos and Scamparini 2004). Seventeen formulations were prepared according to a Central Composite Rotational Design (DCCR 2^3) (Table 1).

Characterization of nanocellulose and nano-biocomposites

Transmission Electronic Microscopy (TEM)

The coconut fiber nanocellulose solution was analyzed by transmission electron microscopy (TEM) to determine the length (L) and diameter (D) of the fibers and to indicate the state of crystal aggregation. The nanocellulose solution was mixed in equal volumes with 2% aqueous uranyl acetate (UA). In total, 10 ml of this mixture was poured in a 400 copper mesh and left to stand for 30-60 s. The mesh was dried and examined on a scanning electron microscope CM12-transmission (STEM) operating in a bright field mode at 80 kV. The lengths and diameters of the crystals were measured directly from the transmission electronic micrographs

*Corresponding author. E-mail: brunamachado17@hotmail.com. Tel (55 71) 38795255. Fax: (55 71) 3879-5255.

Table 1. Real and codified values from the Central Composite Rotational Design (DCCR) of the independent variables: cassava starch (g/100 g; X_1), glycerol (g/100 g; X_2) and coconut cellulose (g/100 g; X_3).

Formulations	Codified Values			Real values (g/100 g)		
	Cassava starch (X_1)	Glycerol (X_2)	Nanocellulose (X_3)	Cassava starch	Glycerol	Nanocellulose
F1	-1.00	-1.00	-1.00	3.60	0.90	0.18
F2	-1.00	-1.00	1.00	3.60	0.90	0.42
F3	-1.00	1.00	-1.00	3.60	2.10	0.18
F4	-1.00	1.00	1.00	3.60	2.10	0.42
F5	1.00	-1.00	-1.00	5.40	0.90	0.18
F6	1.00	-1.00	1.00	5.40	0.90	0.42
F7	1.00	1.00	-1.00	5.40	2.10	0.18
F8	1.00	1.00	1.00	5.40	2.10	0.42
F9	-1.68	0.00	0.00	3.00	1.50	0.30
F10	1.68	0.00	0.00	6.00	1.50	0.30
F11	0.00	-1.68	0.00	4.50	0.50	0.30
F12	0.00	1.68	0.00	4.50	2.50	0.30
F13	0.00	0.00	-1.68	4.50	1.50	0.10
F14	0.00	0.00	1.68	4.50	1.50	0.50
F15*	0.00	0.00	0.00	4.50	1.50	0.30
F16*	0.00	0.00	0.00	4.50	1.50	0.30
F17*	0.00	0.00	0.00	4.50	1.50	0.30

*Central points.

using Image Tool 6.3 (Media Cybernetics, Inc., Bethesda, MD) with 30 measurements to determine the average values and standard deviation (Silva et al., 2012).

Mechanical properties

The tensile test of the nano-biocomposites were conducted using an eletromechanical universal testing machine by EMIC (model DL2000/700) with maximum load of 20 KN following ASTM D-882 (2001) with velocity of 12.5 mm min^{-1} at 25°C. Eight proof bodies were used for each sample to get average value. The proof bodies were of length 80 mm and width 25 mm, and their strength was calculated by dividing the maximum applied force by the area of the film (width × thickness). The strain at breakage was calculated by dividing the final length by the projection of the probe tip (50 mm) and multiplying by 100 (Fakhouri et al., 2013).

Thickness (T)

The film thickness was determined by an average thickness from 6 measurements in random positions using a digital flat-headed micrometer (Mitutoyo; resolution 1 µm) in triplicate.

Water activity (aw) and humidity

The water activity (aw) of the films was measured with a decagon (AQUALAB LITE). The film's humidity was determined by drying using an infrared (Mettler) drying unit (LTJ) by adjusting the radiation intensity emitted until the sample reached 110°C (Veiga-Santos et al., 2005). The analyses were performed in triplicate.

Permeability to water vapor (PWV)

The water vapor permeability of the films was performed through a gravimetric method, recommended by ASTM E96-00 modified (2000). The standard method consisted of successively weighing a capsule with a hermetically sealed surface using the film. The samples were stored with a desiccator substance (silica gel) in its interior and placed in a humidity-controlled environment (desiccator at room temperature ±23°C and 70% relative humidity, using sodium chloride). Water vapor transport (WVT) was determined from the weight gain of the permeation, measuring over 24 h for 10 days. The permeability to water vapor was calculated according to Equation 1 (Famá et al., 2012):

$$\text{Permeability to water vapor} = WVT.e / Po.RH \quad (1)$$

Where, e is the film thickness and Po is the saturation vapor pressure of water at room temperature (Gennadios et al., 1994).

Central composite rotational design (DCCR) and statistical analysis

The films were developed using a central composite rotational statistical design with a 2^3 model containing 4 axial points, 10 orthogonal points and 3 central points, which totaled 17 formulations. The real and the codified values of the independent variables, cassava starch (% m/m; X_1), glycerol (% m/m; X_2) and coconut nanocellulose (% m/m; X_3), which were defined with a process restriction, can be found in Table 1. To evaluate the influence of nanocellulose on the properties of nano-biocomposites, a film of cassava starch without the nanocellulose was used as control and was composed of 4.5% cassava starch and 1.5% glycerol.

The data were treated using a Tukey Test and ANOVA to identify whether the alterations in the evaluated parameters were significant at a 95% significance level. To evaluate the influence of the independent variables, the response surface methodology was used. The second degree polynomial was calculated using the program Statistic 7.0 (Stat Inc, Minneapolis, MN, USA) to evaluate the influence of the independent variables (X_1, X_2 and X_3) on each dependent variable (Y) according to the model generated below (Equation 2):

$$Y=b_0+b_1X_1+b_2X_2+b_3X_3+b_{11}X_1^2+b_{22}X_2^2+b_{33}X_3^2+b_{12}X_1X_2+b_{13}X_1X_3+b_{23}X_2X_3 \quad (2)$$

Where, Y = dependent variable; X_1, X_2 and X_3 = independent variables; b_0 = compensation term; b_1, b_2 and b_3 = linear terms; b_{11}, b_{22} and b_{33} = quadratic terms; and b_{12}, b_{13} and b_{23} = interaction terms among the independent variables.

RESULTS AND DISCUSSION

Characterization of nanocellulose from green coconut fibers

Chemical processes are the primary methods for cellulose nanocrystals isolation from ligno-cellulosic fibers. These methods generally involve washing the fibers with alkaline solutions and bleaching to obtain cellulose, followed by acid hydrolysis using strong acids.

These hydrolysis processes rely on the crystalline regions being insoluble in acids in certain conditions, which is due to the inaccessibility presented by the high organization of the cellulose molecules in their nanostructure. Conversely, the natural disorganization of the cellulose molecules in the amorphous regions favors the accessibility of the acids and consequently the hydrolysis of the cellulose chains present in these regions. Therefore, the isolation of nanocellulose is facilitated by the faster hydrolysis kinetics shown by amorphous regions compared with crystalline regions (Samir et al., 2005).

After four successive phases of treatment with an alkaline solution, the fibers were bleached to intensify the effects of the alkaline treatment, to remove the residual lignin and to increase the exposure of cellulose. After bleaching, the fibers changed from brown to white, as observed in the alkaline treatment, indicating that the bleaching had produced the expected results. For each 10 g of fiber that was washed and bleached, approximately 1.25 g of cellulose was obtained with a 12.5% yield for this extraction from this cellulose; the yield obtained for the production of nanocrystals was 66%.

The cellulose nanocrystals were prepared in an aqueous dispersion (0.033 g/10 mL). Various studies have described the use of faster hydrolysis time periods for obtaining nanocellulose solutions, compared with those used in this study. This indicated that the quantity and percentage of acid as well as the temperature and vigorous agitation all significantly contributed to optimizing the extraction process because the nanocellulose solution was obtained after a short period of hydrolysis.

Rosa et al. (2010) prepared nanocellulose from green coconut fibers (the same matrix used in this study) in faster time frames (120, 150 and 180 min) using the same concentration of H_2SO_4 (64% v/v); however, a lower temperature (45°C) and a smaller proportion of cellulose pulp and acid (10 g/10 ml) was used. Therefore, the method used in the present study (12 ml/g cellulose, 50°C, 10 to 15 min heating) reduced the time for obtaining nanocellulose by a factor of 10 (much shorter time). Silva et al. (2012) also prepared nanocellulose by hydrolysis with H_2SO_4 (64% v/v) from 12 ml/g cellulose pulp from piassaba with constant agitation for 15 to 17 min at 50°C. The acid concentration, temperature and ratio of acid to cellulose pulp used in this study were the same as in the Silva study, which demonstrated that these conditions were favorable for obtaining nanocellulose solutions with a shorter hydrolysis period.

Figure 1 shows the micrographs obtained by the transmission electronic microscopy (TEM) of the nanocrystals from coconut cellulose in an aqueous solution (0.66 g/10 ml). These images provide evidence of the efficiency of the acid hydrolysis treatment to obtain nanocellulose from green coconut fiber. The images also confirm that the aqueous dispersions contain nanocrystals, which primarily consist of individual and some aggregate fibrils. This was consistent with the structural model proposed by Battista and Smith (1962) and with the results obtained by Samir et al. (2005), Rosa et al. (2010), Thomas et al. (2015), Rambabu et al. (2016) and Silva et al. (2012).

The L and D of the cellulose crystals and the relationship of L/D are listed in Table 2. The conditions of hydrolysis used for the preparation of the nanocrystals affected the dimensional properties of these particles (Bondeson et al., 2006). This was because the prolonged acid attack could destroy the amorphous parts of the cellulose and destroy the partially crystalline zones of the fibers, which resulted in a reduction of the nanocrystal length.

The L of the coconut cellulose nanocrystals varied between 98 to 430 nm, and the average D was 6 nm. The average L/D ratio was 38.9±4.7, which was in a good range for use as a support in nano-biocomposites (Rosa et al., 2010). The coconut cellulose nanocrystals obtained with longer hydrolysis time and a lower temperature by Rosa et al. (2010) had an average L and D of 197 and 5.8 nm, respectively, and a L/D ratio of 39. The results found in this study were also consistent with those found by other authors, who characterized the dimensions of nanocellulose from different ligno-cellulosic sources (Bondeson et al., 2006; Elazzouzi-Hafraoui et al., 2008; Roohani et al., 2008; Silva et al., 2012; Rambabu et al., 2016). Methods used to prepare nanocellulose are inexpensive; in addition, green coconut bark is widely

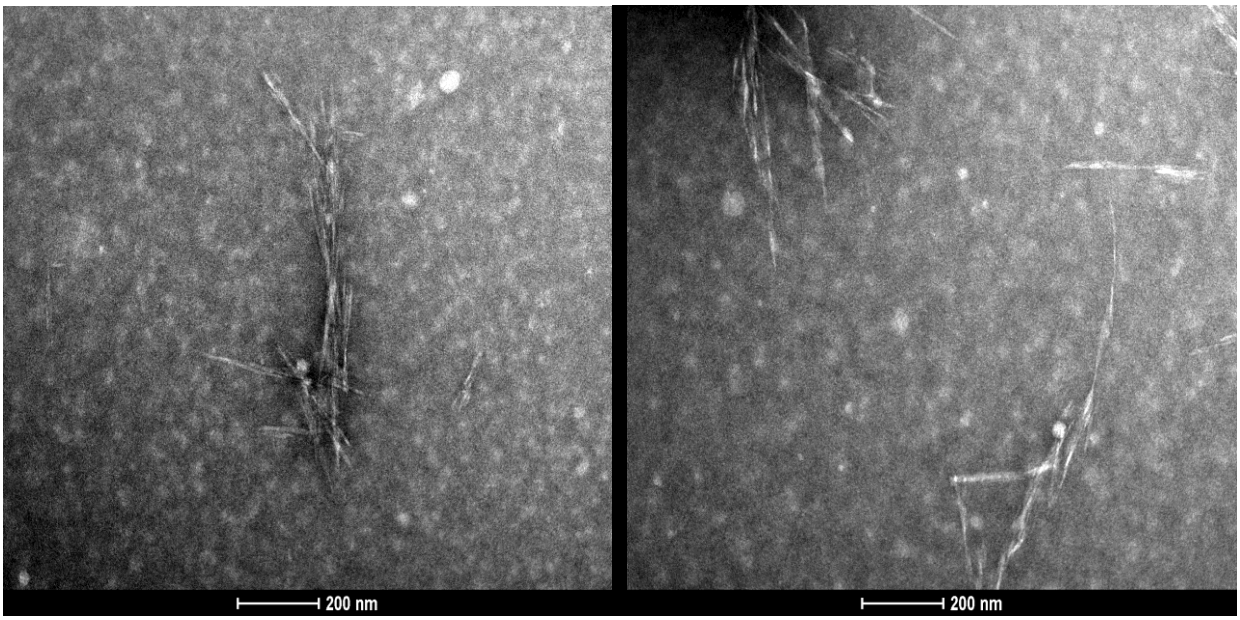

Figure 1. Micrographs obtained (TEM) from the coconut nanocellulose solution, evidencing the presence of nanocrystals (Scales: 200 nm).

Table 2. Dimension of the crystals of nanocellulose from green coconut fibers prepared by acid hydrolysis determined from TEM images.

Length (L –nm)			Thickness (D – nm)	Rate (L/D)	
Minimum	Maximum	Average		Interval	Average
98	430	201±57	5.6±0.98	18.2 – 75.4	38.9±4.7

available, and its disposal is a problem. Thus, green coconut bark can be used as a viable raw material for the preparation of nanocellulose and as a support for nano-biocomposites. Perhaps, the only limitation of the method used is the use of strong acids to obtain the nanocrystals.

Barrier properties of nano-biocomposites

The films were prepared from the values established by the statistical design. Despite drying the 40 g of filmogenic solution in Petri dishes, the resulting thicknesses varied (0.093 mm for formulation F9 to 0.146 mm for formulation F10). Therefore, there were few significant differences between the nano-biocomposite samples ($p<0.05$) (Table 3). The independent variables (percentage of cassava starch, glycerol and nanocellulose) exerted significant effects ($p<0.05$) on the thickness (dependent variable) of the films. As expected, the percentage of starch present in the formulation was primarily responsible for the increase in thickness of the nano-biocomposites. Thus, the differences in film thickness are principally due to the higher solids concentration of the solution.

Water activity (aw) and water content is critical factor for the stability of food. The values of aw varied from 0.638 to 0.710 among the 17 formulations considered in this study, which were lower than the control (0.830). Therefore, these formulations were considered products with intermediate humidity (using classification for foods). According to Table 3, all films that contained coconut nanocellulose showed a significant decrease in the humidity and aw level when compared with the control film. Formulation F11 had the lowest aw (0.638±0.07) and the lowest humidity percentage (15.50±1.22) values. Silva et al. (2012) formulated and characterized starch films containing nanocellulose from eucalyptus and found aw values varying from 0.461 to 0.630. They also verified that the formulations containing the higher percentages of nanocellulose had lower aw values.

The results indicated that the (aw) of starch films plasticized with glycerol can be controlled and improved through the incorporation of nanocellulose from green coconut fibers obtained by acid hydrolysis. Therefore, the addition of these nanocrystals can considerably increase the shelf life of nano-biocomposites through a reduction

Table 3. Average values (± sd – standard deviation) of the dependent variables regarding the barrier properties of the nano-biocomposites and control (C).

F	T ± sd	aw ± sd	TS ± sd	H ± sd	PWV ± sd
Control	0.079±0.03^{a}	0.830±0.21	57.36±1.34	42.64±2.18	9.7x10^{-8}±0.31
F1	0.095±0.01^{a}	0.653±0.18^{a}	84.00±0.92^{a,e,h}	16.00±1.22	6.35x10^{-8}±0.67^{a,g}
F2	0.099±0.02^{b,e,f}	0.657±0.18^{a}	82.64±1.07^{a,e,h,i}	17.36±1.22	5.98x10^{-8}±0.87^{b,c,d,e,f,i}
F3	0.107±0.02^{b,f}	0.710±0.12	68.99±1.33	31.01±2.07	6.33x10^{-8}±0.89^{a}
F4	0.125±0.03^{c,h}	0.692±0.03^{b}	73.14±1.77^{d}	26.86±1.80^{a}	6.01x10^{-8}±0.74^{b,d,f,i}
F5	0.129±0.02^{c}	0.643±0.10^{c}	80.13±0.89^{b,ef,g,h}	19.87±1.21	6.30x10^{-8}±0.71^{a}
F6	0.135±0.01^{g}	0.654±0.09^{a}	80.69±1.13^{b,e,f,g,h,i}	19.31±1.39	5.99x10^{-8}±0.75^{b,c,d,e,f,i}
F7	0.145±0.03^{d}	0.691±0.05^{b}	77.88±1.09^{c,f}	22.12±2.05	6.32x10^{-8}±0.60^{a}
F8	0.146±0.01^{d}	0.674±0.06^{e}	77.50±1.34^{c}	22.50±1.19	6.03x10^{-8}±0.68^{b,f}
F9	0.093±0.02^{e,f}	0.693±0.11^{b}	73.80±2.01^{d}	26.20±2.18	5.95x10^{-8}±0.76^{c,d,e,f,i}
F10	0.146±0.03^{d}	0.685±0.10^{d,f}	81.22±1.85^{e,g,h,i}	18.78±1.49^{b}	5.97x10^{-8} ±0.86^{d,e,f,i}
F11	0.097±0.02^{f}	0.638±0.07^{c}	84.50±1.75	15.50±1.22	5.94x10^{-8} ±0.93^{e,f,h,i}
F12	0.139±0.01^{g}	0.693±0.09^{b}	71.17±1.62	28.83±1.09^{a}	5.98x10^{-8}±0.77^{f,i}
F13	0.119±0.03^{h,i,j,l}	0.680±0.10^{d,e,f}	79.42±1.55^{f,g}	20.58±1.12	6.40x10^{-8}±0.66^{g}
F14	0.122±0.02^{h,i,l}	0.676±0.12^{e,f}	80.39±1.19^{g,h,i}	19.61±0.18	5.89x10^{-8}±0.91^{h}
F15*	0.117±0.02^{i,j,l}	0.683±0.15^{d,f}	81.21±1.33^{h,i}	18.79±1.45^{b}	5.97x10^{-8}±0.81^{i}
F16*	0.116±0.01^{j,l}	0.680±0.05^{f}	81.92±1.32^{i}	18.08±1.60	5.94x10^{-8} ±0.86^{i}
F17*	0.119±0.03^{l}	0.682±0.08^{f}	81.72±1.24^{h,i}	18.28±1.85	5.93x10^{-8} ±0.81^{i}

Formulations (F) of DCCR; *Central Points. Values presenting the same letter, in the same column, do not show significant differences ($p>0.05$) by the Tukey Test at 95% confidence level. T, thickness - mm; aw, water activity; TS, total solids - %; H, humidity (%); PWV, permeability to water vapour - $gH_2O/m.s.Pa$.

in water quantity available for microorganism growth and for the occurrence of chemical reactions.

Total solids, humidity and water activity were significantly affected ($p<0.05$) by three independent variables. The plasticizer glycerol exerted the most significant effect ($p<0.05$) on three parameters. It had a negative effect on the total solids content and a positive effect on the humidity and aw values. Glycerol is a hydrophilic plasticizer that interacts with water to form hydrogen bonds, thus interfering with values of the aw and humidity of nano-biocomposites.

When glycerol was used under low concentrations, the films showed low values of water activity and humidity. The anti-plasticizing effect has already been reported by other authors when evaluating this plasticizer in different combinations and with other types of starch (Gaudin et al., 2000; Chang et al., 2006; Mali et al., 2008; Liu et al., 2013). Balakrishnan et al. (2017) evaluated potato starch films with pineapple nanocellulose, from the results, it was assumed that the starch glycerol system exhibits a heterogenous nature and cellulose nanofibers tend to move towards glycerol rich starch phase. Barrier properties also improved with the addition of nano-cellulose up to 3 wt% but further addition depreciated properties due to possible fiber agglomeration. Formulations F1, F2, F5 and F6 containing 0.9% of the plasticizer, and F11, with 0.5%, showed lower values of humidity and aw when compared with the other formulations and the control.

The incorporation of nanocellulose in the polymeric matrix of cassava starch with glycerol resulted in a decrease in the values of water vapor permeability, which varied from 5.89x10^{-8} to 6.40x10^{-8} $gH_2O/m.s.Pa$. This was much lower than the control (9.7x10^{-8} $gH_2O/m.s.Pa$) (Table 3). Formulation F13, which had a lower percentage of nanocellulose (0.1% m/m), showed the higher permeability among the nano-biocomposites studied (6.40x10^{-8} $gH_2O/m.s.Pa$), whereas F14, which had the highest percentage of nanocellulose (0.5% m/m) showed the lower value (5.89x10^{-8} $gH_2O/m.s.Pa$). Therefore, there was a decrease of 34 and 39.3% in the water vapor permeability for F13 and F14, respectively, compared with the control film. The presence of the cellulose nanocrystals in the matrix in any concentration promoted a reduction in the water vapor permeability, which led to alterations in the nano-biocomposite structures. This reduction in water vapor permeability occurs because the nanocrystals, when associated with glycerol, act as a barrier and decrease the free spaces in the polymeric matrix and impair the passage of vapor (Rosa et al., 2010; de Mesquita et al., 2011; Müller et al., 2008). Besides that, it is supposed that nanocrystals interact through hydrogen bridges with starch chains. Similar results regarding the decrease in water vapor permeability have been determined by Azeredo et al. (2009) when incorporating nanocrystals of commercial cellulose in

mango puree films. Thus, coconut cellulose nanocrystals used as a physical barrier to water permeability can be explained by the high degree of crystallinity of the nanoparticles, which present a crystallinity index of approximately 70% (calculated through the analysis of X-ray diffraction – DRX – data not shown). The crystallinity of the cellulose nanoparticles have also been used to explain the decrease in the water vapor permeability rate and water solubility in PWV membranes (Paralikara et al., 2008), Xylan membranes (Saxena and Ragauskas, 2009) and starch films plasticized with sucrose and inverted sugar (Silva et al., 2012) incorporated with nanocrystals. Water transport in edible films based on hydrophilic materials such as starch, is a complex phenomenon due to the strong interaction of sorbed water molecules with the polymeric structure. Slavutsky and Bertuzzi (2014) identified that the measured film solubility, contact angle, and water sorption isotherm indicated that reinforced starch/nanocellulose films have a lower affinity to water molecules than starch films. The interaction between nanocellulose and starch chain is favoured by the chemical similarities of both molecules.

The statistical study showed that the independent variables exerted a significant effect ($p<0.05$) based on the concentration of nanocellulose (L and Q), glycerol (Q) and starch (Q) on the PWV (permeability to water vapor) of the nano-biocomposites, which were represented by quadratic and linear functions. The concentration of coconut nanocellulose directly influenced the permeability to water vapor; as the concentration of these nano-particles increased in nano-biocomposites, the permeability to water vapor decreased ($R^2= 0.98$) (Figure 2). Similar results to this study were found by Lu et al. (2005), Wang et al. (2006) and Cao et al. (2008) for nano-biocomposites with starch, protein and starch matrixes, respectively, containing nanocellulose from cotton linter (Lu et al., 2006) and from hemp (Cao et al., 2008).

The analysis of the experimental data for the different formulations resulted in polynomial second order equations for each response surface generated: thickness (T), total solids (TS), humidity (H), water activity (aw) and permeability to water vapor (PWV) (Table 4). Through the use of these equations, it is possible to optimize each independent variable concentration to obtain a better response in relation to the barrier properties, assisting future studies.

Mechanical properties of the films

The incorporation of a coconut nanocellulose solution to biodegradable films of cassava starch plasticized with glycerol in different concentrations resulted in alterations of the mechanical properties of all formulations studied (Table 5). The coconut cellulose nanocrystals, combined with other independent variables were efficient in increasing the maximum tension. An increase of up to 1.619% (F11) was observed compared with the control (starch film without nanocellulose). This property was significantly altered ($p<0.05$) with the incorporation of nanocellulose in all concentrations studied (0.1 to 0.5%).

The value of the Young's modulus (elasticity) also increased significantly ($p<0.05$) with the incorporation of nanocellulose. Formulations F10, F6 and F11 showed an increase of 3.419, 5.525 and 47.090%, respectively, in this parameter compared with the control film. However, there was a decrease of deformation in the rupture (ε) of all of the formulations containing coconut nanocellulose, which was expected. This was most likely due to the increase in rigidity of the nano-biocomposites, which showed a decrease in the ductile capacity of the nanomaterial. This behavior is usually expected when a more rigid component – in this case the nanoparticles of cellulose – is added to a more flexible material (the starch).

This effect can be attributed to the phenomenon known as the mechanical percolation of cellulose nanocrystals and the formation of a continuous network of nanocellulose linked by hydrogen interactions. Alternatively, it could have been due to a good dispersion of the nanocrystals in the matrix, which would indicate a good interaction among the components of the film that could be proven with images of nanoparticle distribution inside the film by electron microscopy. Samir et al. (2005) have reported that cellulose nanocrystals are regions that grow under controlled conditions, which allow for the formation of individual crystals of high purity. This highly ordered structure could show high resistance and significant changes in some important properties of the materials, such as electrical, optical, magnetic, ferromagnetic, dielectric and conductivity.

Chaichi et al. (2017) developed edible pectin film reinforced by crystalline nanocellulose and the incorporation of three levels of nanocellulose (2, 5 and 7% w/w) on mechanical and water vapor barrier properties of pectin-based biodegradable film were investigated. The optimum result was obtained through the nanocomposite film with 5% nanocellulose in terms of mechanical and water vapor properties as the tensile strength increased up to 84% and water vapor permeability decreased by 40%. Cao et al. (2008) reported similar results to this study when they formulated and mechanically characterized biodegradable films of thermoplastic starch and nanocellulose from hemp fibers as a support material. The resistance (maximum tension) increased from 3.9 to 111.5 MPa when the content of nanocellulose increased from 0 to 30%. For the same concentrations of nanocellulose, the Young's modulus increased from 31.9 to 823.9 MPa, respectively. Wang et al. (2010) developed starch nano-composites and polyurethane with varied concentrations of nanocellulose through casting and reported that the incorporation of 1% nanocellulose in the matrix increased

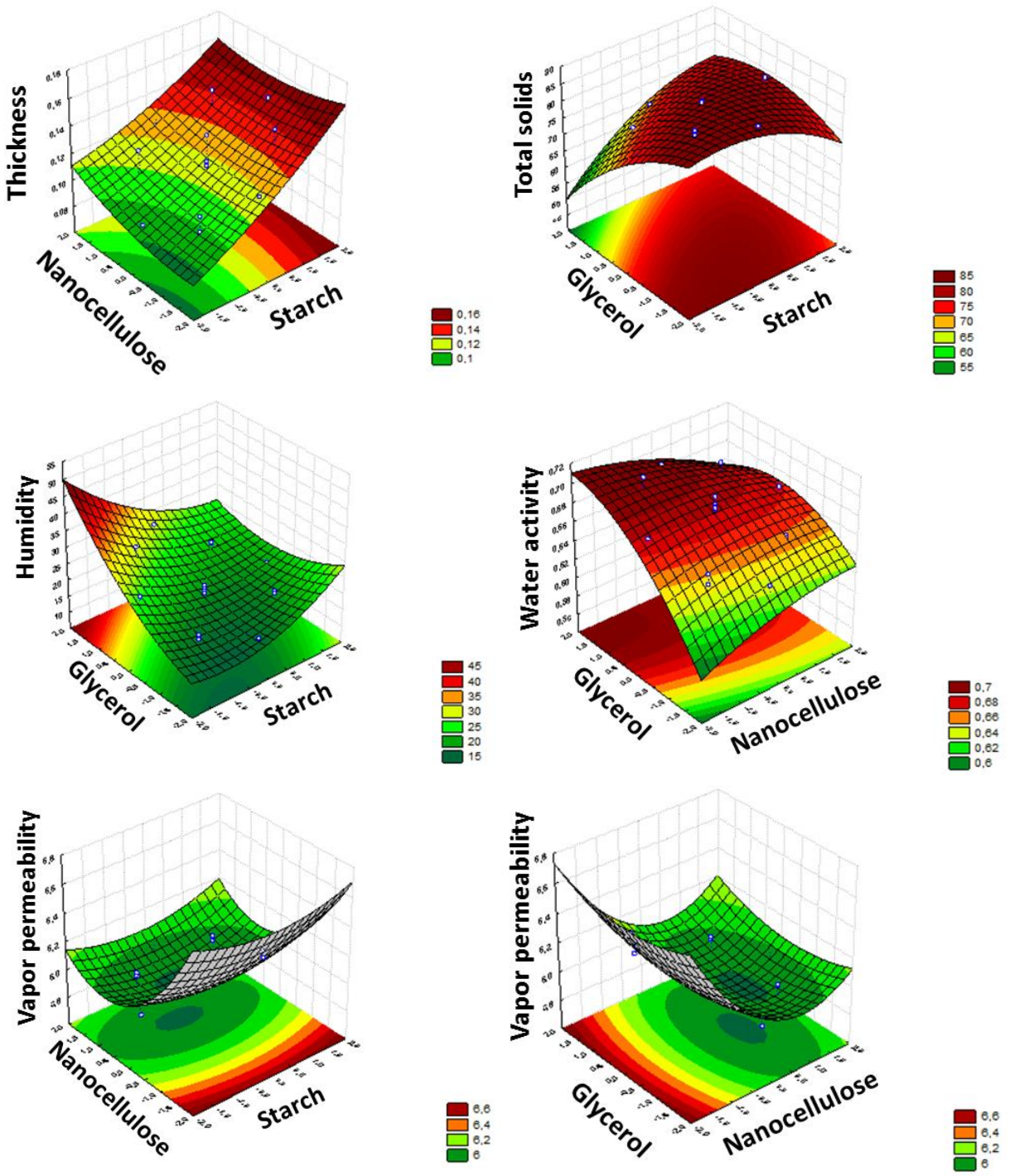

Figure 2. Response surfaces generated for the interactions of the independent variables (starch, glycerol and nanocellulose) on the dependent variables: thickness, total solids, humidity, water activity (aw) and water vapor permeability (PWV) of the 17 formulations of nano-biocomposites.

the resistance to tensile of the nanocomposites from 5.4 to 12.7 MPa (135%), the Young's modulus from 0.5 to 1.8 MPa (252%), and the rupture tension from 35.8 to 84.6 MPa (136%), compared with the control. Montero et al. (2017) reported that the incorporation of cellulose nanoparticles favoured plasticization and increased the rigidity in thermoplastic starches films and moisture resistance. Azeredo et al. (2009) prepared edible films

Table 4. Equations of the model and R^2 (determination coefficient) for thickness (T, mm), total solids (TS, %), humidity (H, %), Water Activity (aw), Permeability to water vapor (PWV, $gH_2O/m.s.Pa$) of the films, X_1= Cassava starch, X_2= Glycerol and X_3= Coconut nanocellulose.

Parameters (Independent variables *versus* Independent variables)	Equation	R^2
Thickness (X_1 *versus* X_3)	$0.117 + 0.015X_1 + 0.014X_1^2 + 0.024X_3 + 0.001X_3^2 – 0.001X_1X_3$	0.97
Total Solids (X_1 *versus* X_2)	$81.62 + 1.458X_1 – 1.474X_1^2 – 3.834X_2 – 1.359X_2^2 – 2.387X_1X_2$	0.97
Humidity (X_1 *versus* X_2)	$18.37 – 1.458X_1 + 1.474X_1^2 + 3.834X_2 + 1.359X_2^2 – 2.387X_1X_2$	0.97
Water activity (X_2 *versus* X_3)	$0.682 + 0.018X_3 – 0.006X_3^2 – 0.019X_2 – 0.002X_2^2 – 0.006X_2X_3$	0.97
PWV (X_1 *versus* X_3)	$5.939 + 0.004X_1 + 0.029X_1^2 – 0.138X_3 + 0.096X_3^2 – 0.003X_1X_3$	0.98
PWV (X_2 *versus* X_3)	$5.939 + 0.012X_3 + 0.029X_3^2 – 0.138X_2 + 0.096X_2^2 + 0.003X_2X_3$	0.98

Table 5. Average values (± sd – standard deviation) of the dependent variables regarding the mechanic properties of the nano-biocomposites and control (C) and percentage of alterations in relation to control.

F	E (MPa)	↑E (%)	σ (MPa)	↑ σ (%)	ε (%)	↓ ε (%)
Control	1.00±0.24	-	0.87±0.12[f]	-	100.44±4.05	-
F1	26.71±1.41	2.670	2.81±0.11	323	71.72±1.01	28.6
F2	29.19±0.97	2.919	3.01±0.32	346	68.38±1.75	31.9
F3	4.56±0.32[a]	456	0.91±0.07[a,f]	105	29.00±0.89	71.1
F4	5.89±0.83	589	1.03±0.10[a,c]	118	27.91±1.30	72.2
F5	13.25±1.52[b]	1.325	1.89±0.21[b,d]	217	59.02±1.17	41.2
F6	55.25±7.20	5.525	3.82±0.36	439	14.91±1.11	85.15
F7	10.98±0.95	1.098	1.59±0.08	183	40.00±1.01	60.2
F8	15.09±1.06[c]	1.509	1.91±0.15[b,d]	219	38.36±0.91	61.8
F9	4.81±0.65[a,d]	481	1.01±0.11[a,c]	116	40.86±1.13	59.3
F10	34.19±1.13	3.419	3.22±0.41	370	56.18±1.20	55.9
F11	470.90±9.07	47.090	14.09±1.22	1.619	6.01±0.43	94.0
F12	4.89±0.43[a]	489	1.06±0.03[c]	122	89.02±1.54	11.4
F13	13.93±0.90[b]	1.393	1.81±0.89[d]	208	37.54±1.21	62.6
F14	18.98±1.21	1.898	4.02±0.18	462	37.98±0.87	62.2
F15*	15.04±0.76[c,d]	1.504	2.45±0.35[e]	281	50.29±1.09[a]	50.1
F16*	14.94±1.45[c,d]	1.494	2.05±0.64[e]	277	49.16±0.98[a]	51.0
F17*	15.13±0.82[d]	1.513	2.42±0.65[e]	278	50.36±1.22[a]	49.9

Formulations (F); *Central Points. ↑ or ↓: increase in relation to control. Values that show the same letter, in the same column, do not have significant differences ($p>0.05$) by the Tukey Test at 95% confidence level. E, Young Module (MPa); σ, maximum tension (MPa); ε, deformation (%).

from mango puree that were strengthened with nanofibers of commercial cellulose. They observed that the nanocrystals were efficient in increasing the resistance to tensile, and this effect on the Young's modulus was even more noticeable at higher concentrations, which suggests the formation of a fibrillar structure inside the matrix.

Cellulose nanocrystals obtained from any natural source, are responsible for improving the mechanic properties of films when incorporated into the films that are composed of either biodegradable or synthetic matrixes. However, in this study, the incorporation of nanocellulose could not be observed as an exclusive parameter because the formulations were prepared with simultaneous variations of two other components, starch and glycerol. According to the Pareto graphs for tension and modulus (Figure 3), the plasticizer glycerol also played an important role in improving the mechanic properties of the studied nano-biocomposites. Glycerol is a small molecule that facilitates its insertion within the polymer chains, exerting a higher influence in their mechanic properties. The polar groups (-OH) of the plasticizer molecules incur plasticizer-polymer interactions in substitution of the polymer-polymer interactions in the polymeric mixtures. Additionally, the starch underwent a structural modification after a thermal treatment facilitated the interaction of glycerol with its chain and allowed a

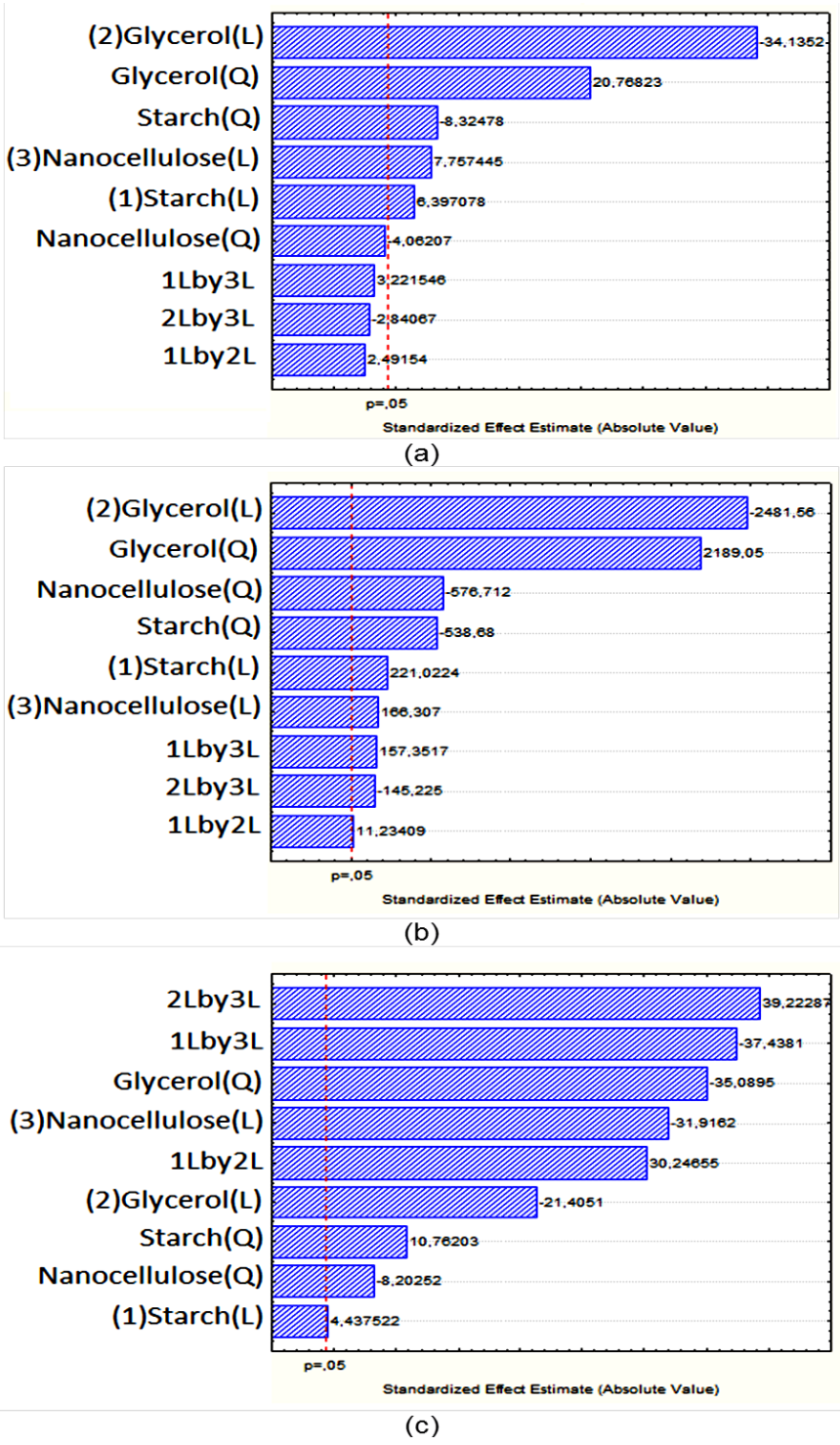

Figure 3. Pareto graphs for (a) module, (b) tension and (c) deformation of the nano-biocomposites.

greater interaction between plasticizer-starch-nanocellulose; thus, this contributed to improving the mechanic properties of the films. Therefore, the incorporation of nanocrystals modifies the mechanical properties, despite the presence or absence of the plasticizer.

Generally, the plasticized films with higher glycerol concentrations are more flexible and have higher

elongation values, whereas the films with lower plasticizer content showed higher modulus and tension values. Glycerol is a hydrophilic plasticizer that interacts with the starch chains, increasing the molecular mobility and consequently the hydrophilicity and flexibility of the plasticized films (Mali et al., 2004). Formulation F11 showed the highest modulus and tension values, whereas F12 had the highest elongation value. These results showed the efficiency of glycerol as a plasticizer, which was also proved in studies for films manufactured with starch by Shimazu et al. (2007), with lactoglobulin by Sothornvit and Krochta (2001) and with soy protein by Cho and Rhee (2002). Azeredo et al. (2010) have demonstrated that lower concentrations of glycerol and higher concentrations of commercial cellulose nano-crystals provide an increase in the mechanic properties of the films obtained from chitosan. According to the Pareto graph (Figure 3), the concentrations of glycerol (X_2) and nanocellulose (X_3) exerted a higher effect on the maximum tension value, whereas the linear interactions between glycerol (X_2) and nanocellulose (X_3) (2Lby3L), and starch (X_1) and nanocellulose (X_3) (1Lby3L) were the primary factors responsible for the deformation percentage (elongation) of the nano-biocomposites.

The nano-biocomposites examined in this study can be considered complex systems that showed competitive interactions among all the present components in variable concentrations. The incorporation of nano-cellulose from coconut was determined as efficient in decreasing the water permeability of the films and improving the mechanic properties of the system and thus widening the applications of nanocellulose from coconut materials. Finally, the isolation of cellulose nanocrystals constitutes an excellent alternative to the reutilization of ligno-cellulosic residues and their application as support additives in polymeric materials.

Conclusion

The results shown in this study demonstrate that it is possible to obtain nanocellulose from green coconut fibers through the process of acid hydrolysis (H_2SO_4 64%, 50°C, 10-15 min) with an L/D ratio of 38.9±4.7. The incorporation of these nanocrystals in cassava starch films plasticized with glycerol contributes to significantly improving the mechanical properties of films, such as Young's modulus and maximum tension. These effects consequently decrease the elongation percentage of the films. When compared with the controls, all formulations showed an increase in the Young's modulus. Formulation F11 reached the upper limit with an approximate 47.000% increase and a consequent decrease in elongation of 94% compared with the control. In addition, the presence of nanocrystals in the polymeric matrix of starch improved the barrier properties, such as water vapor permeability and water activity of the films.

Therefore, films formulated from cassava starch and plasticized with glycerol can have their mechanic and barrier properties significantly altered by the incorporation of coconut cellulose.

CONFLICT OF INTERESTS

The authors have not declared any conflict of interests.

ACKNOWLEDGEMENTS

The authors would like to thank the *Fundação de Amparo a Pesquisa do Estado da Bahia* (Fapesb) for the financial support towards the research.

REFERENCES

ASTM-American Society for Testing and Materials (2000). Standard test methods for water vapor transmission of materials. Annual Book of ASTM Standards. Designation E96-00.

Azeredo HMC, Mattoso LHC, Avena-Bustillos RJ, Ceotto-Filho G, Munford ML, Wood D, McHugh TH (2010). Nanocellulose Reinforced Chitosan Composite Films as Affected by Nanofiller Loading and Plasticizer Content. J. Food Sci. 75(1):1-7.

Azeredo HMC, Mattoso LHC, Wood D, Williams TG, Avena-Bustillos RJ, McHugh TH (2009). Nanocomposite Edible Films from Mango Puree Reinforced with Cellulose Nanofibers. J. Food Sci. 74(5):31-35.

Balakrishnan P, Sreekala MS, Kunaver M, Huskić M, Thomas S (2017). Morphology, transport characteristics and viscoelastic polymer chain confinement in nanocomposites based on thermoplastic potato starch and cellulose nanofibers from pineapple leaf. Carbohydr. Polym. 169:176-188.

Bondeson D, Mathew A, Oksman K (2006). Optimization of the isolation of nanocrystals from microcrystalline cellulose by acid hydrolysis. Cellulose 13(2):171-180.

Cao X, Chen Y, Chang PR, Stumborg M, Huneault MA (2008). Green Composites Reinforced with Hemp Nanocrystals in Plasticized Starch. J. Appl. Polym. Sci. 1(109):3804-3810.

Chaichi M, Hashemi M, Badii F, Mohammadi A (2017). Preparation and characterization of a novel bionanocomposite edible film based on pectin and crystallinenanocellulose. Carbohydr. Polym. 157(10):167-175.

Chang YP, Karim AA, Seow CC (2006). Interactive plasticizing-antiplasticizing effects of water and glycerol on the tensile properties on tapioca starch films. Food Hydrocoll. 20(1):1-8.

Cho SY, Rhee C (2002). Sorption characteristics of soy protein films and their relation to mechanical properties. LWT Food Sci. Technol. 35(2):151-157.

Costa SS, Druzian JI, Machado BAS, Souza CO de, Guimarães AG (2014). Bi-Functional Biobased Packing of the Cassava Starch, Glycerol, Licuri Nanocellulose and Red Propolis. PloS One 9(11):e112554.

Costa SS, Silva RPD, Alves ARC, Guarieiro LLN, Machado BAS (2016). Prospective Study on the Collection and Incorporation of Cellulose Nanocrystals in Biodegradable Films. Rev. Virtual Quim. 8(4):1104-1114.

de Mesquita JP, Patrício PS, Donnici CL, Petri DF, de Oliveira LC, Pereira FV (2011). Hybrid layer-by-layer assembly based on animal and vegetable structural materials: multilayered films of collagen and cellulose nanowhiskers. Soft Matter 7(1):4405-4413.

Elazzouzi-Hafraoui S, Nishiyama Y, Putaux JL, Heux L, Dubreuil F,

Famá L, Gañan-Rojo P, Bernal C, Goyanes S (2012). Biodegradable starch based nanocomposites with low water vapor permeability and high storage modulus. Carbohydr. Polym. 87(3):1989-1993.

Gaudin S, Lourdin D, Forssell PM, Colonna P (2000). Antiplasticisation and oxygen permeability of starchsorbitol films. Carbohydr. Polym. 43(1):33-37.
Gennadios A, Weller CL, Gooding CH. Measurement errors in water vapor permeability of highly permeable, hydrophilic edible. J. Food Eng. 21(1):395-409
Henrique CM, Teófilo RF, Sabino L, Ferreira MMC, Cereda MP (2007). Classification of Cassava Starch Films by Physicochemical Properties and Water Vapor Permeability Quantification by FTIR and PLS. J. Food Sci. 72(4):E184-E189.
Kermit PD (2010). Improved fiber reinforced plastic composites and method and apparatus for making. Patent Espacenet US 2010004632.
Kun CM (2011). Extrusion machine for manufacturing Wood fiber plastic composites. Patent Espacenet KR 20110059333.
Li C, Liu H, Luo B, Wen W, He L, Liu M, Zhou C (2016). Nanocomposites of poly(L-lactide) and surface-modified chitin whiskers with improved mechanical properties and cytocompatibility. Euro. Polym. J. 81(1):266-283.
Liu D, Dong Y, Bhattacharyya D, Sui G (2017). Novel sandwiched structures in starch/cellulose nanowhiskers (CNWs) composite films. Composites Communications 4(1):5-9.
Liu H, Adhikari R, Guo Q, Adhikari B (2013). Preparation and characterization of glycerol plasticized (high-amylose) starch–chitosan films. J. Food Eng. 116(2):588-597.
Lu Y, Weng L, Cao X (2005). Biocomposites of Plasticized Starch Reinforced with Cellulose Crystallites from Cottonseed Linter. Macromol. Biosci. 5(11):1101-1107.
Machado BAS, Reis JHO, Silva JBA, Cruz LS, Nunes IL, Pereira FV, Druzian JI (2014). Obtaining nanocellulose from green coconut fibers and incorporation in biodegradable films of starch plasticized with glycerol. Quím. Nova 37(8):1275-1282.
Mali S, Grossmann MVE, García MA, Martino MM, Zaritzky NE (2004). Barrier, mechanical and optical properties of plasticized yam starch films. Carbohydr. Polym. 56(2):129-135.
Mali S, Grossmann MVE, García MA, Martino MM, Zaritzky NE (2008). Antiplasticizing effect of glycerol and sorbitol on the properties of cassava starch films. Braz. J. Food Technol. 11(3):194-200.
Meneguin AB, Cury BSF, Santos AM, Franco DF, Barud HS, Silva EC (2017). Resistant starch/pectin free-standing films reinforced with nanocellulose intended for colonic methotrexate release. Carbohydr. Polym. 157(1):1013-1023.
Montero B, Rico M, Rodríguez-Llamazares S, Barral L, Bouza R (2017). Effect of nanocellulose as a filler on biodegradable thermoplastic starch films from tuber, cereal and legume. Carbohydr. Polym. 157(1):1094-1104.
Müller CMO, Yamashita F, Laurindo JB (2008). Evaluation of the effects of glycerol and sorbitol concentration and water activity on the water barrier properties of cassava starch films through a solubility approach. Carbohydr. Polym. 72(1):82-87.
Myllytie P, Salmén L, Haimi E, Laine J (2010). Viscoelasticity and water plasticization of polymer-cellulose composite films and paper sheets. Cellulose 17(2):375-385.
Niu F, Li M, Huang Q, Zhang X, Pan W, Yang J, Li J (2017). The characteristic and dispersion stability of nanocellulose produced by mixed acid hydrolysis and ultrasonic assistance. Carbohydr. Polym. 165(1):197-204.
Ortega A, Baillie D (2011). Fiber-Reinforced Plastic Parts Made With Untreated Embossed Surfacing Veils With No Whitening Agents. Patent Espacenet US 2011236638.
Panaitescu DM, Frone AN, Ghiurea M, Chiulan I (2015). Influence of storage conditions on starch/PVA films containing cellulose nanofibers. Ind. Crops Prod. 70(1):170-177.
Paralikara SA, Simonsen J, Lombardi J (2008). Poly(vinyl alcohol)/cellulose nanocrystal barrier membranes. J. Memb. Sci. 320(1-2):248-58.
Qazanfarzadeh Z, Kadivar M (2016). Properties of whey protein isolate nanocomposite films reinforced with nanocellulose isolated from oat husk. Int. J. Biolog. Macromol. 91(1):1134-1140.
Qin Y, Zhang S, Yu J, Yang J, Xiong L, Sun Q (2016). Effects of chitin nano-whiskers on the antibacterial and physicochemical properties of maize starch films. Carbohydr. Polym. 147(1):372-378.
Rambabu N, Panthapulakkal S, Sain M, Dalai AK (2016). Production of nanocellulose fibers from pinecone biomass: Evaluation and optimization of chemical and mechanical treatment conditions on mechanical properties of nanocellulose films. Ind. Crops Prod. 83:746-754.
Rochas C (2008). The Shape and Size Distribution of Crystalline Nanoparticles Prepared by Acid Hydrolysis of Native Cellulose. Biomacromolecules 9(1):57-65.
Roohani M, Habibi Y, Belgacem NM, Ebrahim G, Karimi AN, Dufresne A (2008). Cellulose whiskers reinforced polyvinyl alcohol copolymers nanocomposites. Eur. Polym. J. 44(8):2489-2498.
Rosa MF, Medeiros ES, Malmonged JA, Gregorskib KS, Wood DF, Mattoso LHC, Glenn G, Orts WJ, Imam SH (2010). Cellulose nanowhiskers from coconut husk fibers: Effect of preparation conditions on their thermal and morphological behavior. Carbohydr. Polym. 81(1):83-92.
Rusmirović JD, Ivanović JZ, Pavlović VB, Rakić VM, Rančić MP, Djokić V, Marinković AD (2017). Novel modified nanocellulose applicable as reinforcement in high-performance nanocomposites. Carbohydr. Polym. 164(1):64-74.
Samir MASA, Aloin F, Dufresne A (2005). Review of Recent Research into Cellulosic Whiskers, Their Properties and Their Application in Nanocomposite Field. Biomacromolecules 6(2):612-626.
Saxena A, Ragauskas AJ (2009). Water transmission barrier properties of biodegradable films based on cellulosic whiskers and xylan. Carbohydr. Polym. 78(2):357-360.
Seligra PG, Jaramillo CM, Famá L, Goyanes S (2016). Biodegradable and non-retrogradable eco-films based on starch–glycerol with citric acid as crosslinking agent. Carbohydr. Polym. 138(1):66-74.
Shimazu AA, Mali S, Grossmann MVE (2007). Plasticizing and antiplasticizing effects of glycerol and sorbitol on biodegradable cassava starch films. Cienc. Agrar. 28(1):79-88.
Silva JBA, Pereira FV, Druzian JI (2012). Cassava Starch-Based Films Plasticized with Sucrose and Inverted Sugar and Reinforced with Cellulose Nanocrystals. J. Food Sci. 77(6):14-19.
Silva R, Haraguchi SK, Muniz EC, Rubira AF (2009). Applications of lignocellulosic fibers in polymer chemistry and in composites. Quim. Nova 32(3):661-671.
Sohei S, Hajime T, Michihito M, Kazuki K, Yuhei A, Takahiro M, Ichiya T (2011). Fiber reinforced plastic molding, production method therefor, and elevator. Patent Espacenet, WO 2011122179.
Strurcova A, Stephen J, Eichhorn SJ, Jarvis MC (2006). Vibrational Spectroscopy of Biopolymers Under Mechanical Stress: Processing Cellulose Spectra Using Bandshift Difference Integrals. Biomacromolecules 7(9):2688-2691.
Sun F, Nordli HR, Pukstad B, Gamstedt EK, Chinga-Carrasco G (2017). Mechanical characteristics of nanocellulose-PEG bionanocomposite wound dressings in wet conditions. J. Mech. Behav. Biomed. Mater. 69(1):377-384.
Thomas MG, Abraham E, Jyotishkumar P, Maria HJ, Pothen LA, Tomas S (2015). Nanocelluloses from jute fibers and their nanocomposites with natural rubber: Preparation and characterization. Int. J. Biol. Macromol. 81:768-777.
Veiga-Santos P, Oliveira LM, Cereda MP, Alves AJ, Scamparini ARP (2005). Mechanical properties, hydrophilicity and water activity of starch-gum films: Effect of additives and deacetylated xanthan gum. Food Hydrocoll. 19(2):341-349.
Veiga-Santos P, Scamparini ARP (2004). Indicador irreversível de temperatura utilizando carboidratos. Patent INPI BR PI0403610-7.
Wang Q, Chen S, Chen D (2017). Preparation and characterization of chitosan based injectable hydrogels enhanced by chitin nano-whiskers. J. Mech. Behav. Biomed. Mater. 65(1):466-477.
Wang Y, Cao X, Zhang L (2006). Effects of Cellulose Whiskers on Properties of Soy Protein Thermoplastics. Macromol. Biosci. 6(7):524-531.
Wang Y, Tian H, Zang L (2010). Role of starch nanocrystals and cellulose whiskers in synergistic reinforcement of waterborne polyurethane. Carbohydr. Polym., 80(3):665–671.
Zhong Y, Li Y, Zhao Y (2012). Physicochemical, Microstructural, and Antibacterial Properties of β-Chitosan and Kudzu Starch Composite Films. J. Food Sci. 77(10):280-286.

academicJournals

Vol. 16(28), pp. 1579-1589, 12 July, 2017
DOI: 10.5897/AJB2017.15991
Article Number: 2B7761765096
ISSN 1684-5315

http://www.academicjournals.org/AJB

African Journal of Biotechnology

Full Length Research Paper

Quantitative trait loci for resistance to spotted and African maize stem borers (*Chilo partellus* and *Busseola fusca*) in a tropical maize (*Zea mays* L.) population

Munyiri, S. W.[1*] and Mugo, S. N.[2]

[1]Chuka University, P. O. Box 109-60400, Chuka, Kenya.
[2]International Maize and Wheat Improvement Center (CIMMYT), P. O. Box 1041-0062, Nairobi, Kenya.

Received 16 March, 2017; Accepted 29 June, 2017

Maize (*Zea mays* L.) is the staple food in Kenya, and mapping the qualitative trait loci (QTL) associated with resistance to maize stem borer pest is important towards marker assisted breeding for this quantitative trait. The objective of this study was to identify any QTL associated with resistance to *Chilo partellus* and *Busseola fusca*, the two important stem borer pests in maize production in Kenya. A total of 203 $F_{2:3}$ individuals from a cross between CML442, a stem borer susceptible maize inbred line and CKSBL10026, a stem borer resistant maize inbred line; and 152 SNPs were used for mapping the QTL. Data were collected on leaf damage, stem borer exit holes and stem tunneling length as putative stem borer damage traits. A likelihood odds ratio (LOD) scores of 3.0 and maximum recombination frequency of 0.50 were used to declare linkage. LOD scores between 2.5 and 2.9 were considered strong indications of a QTL. Resistance QTL for the three putative traits were detected on chromosomes 1-7 and 9 for both individual locations and stem borer species analysis. In *B. fusca* sites, one QTL for reduced stem tunnelling was revealed on chromosome 4 while in the *C. partellus* sites, one QTL for reduced stem tunnelling was identified on chromosome 4 and another for reduced stem borer exit holes was identified on chromosome 5. Phenotypic variances explained ranged from 6 to 10%, suggesting a need to validate these QTL using a larger population and in different environments.

Key words: *Busseola fusca*, *Chilo partellus*, mapping, quantitative trait loci (QTL), resistance, single nucleotide polymorphisms (SNPs), stem borer.

INTRODUCTION

Insect pests affect 46% of global maize growing area causing about 24.5% of world maize loss annually. In economic terms, 52 million tons of grain valued at $5.7 billion is lost, and US $550 million worth of insecticide is

*Corresponding author. E-mail: munyirishelmith@yahoo.co.uk. Tel: +254 722 269 532.

used annually to curb losses (Mugo et al., 2012). Annual losses due to pests in Africa are about 17%. Maize stem borer species are the primary field pests that feed on leaves, cob and pith resulting in stem damage and grain yield losses in the entire world wherever maize is grown (Mihm, 1997; Samayoa et al., 2015a). The stem borer pest is also one of the most important maize field pests in sub-Saharan Africa (Kfir et al., 2002; Smale et al., 2011; Calatayud et al., 2014). Increased maize productivity beyond the current two (2) tons per hectare is critical for food security in sub- Saharan Africa. The stem borers are some of the major pests that account for the low maize production, with lepidopteran stem borers, including the African stem borer (*Busseola fusca* Fuller), the spotted stem borer (*Chilo partellus* Swinhoe) and the pink stem borer (*Sesamia Calamistis* Hampson) being the most damaging pests in eastern and southern Africa, where they cause 13 to 40% yield losses (De Groote, 2002; Mailafiya et al., 2011). In Kenya, the major maize stem borer species are *C. partellus*, *B. fusca* and *S. calamistis. C. partellus* is found in the warmer and lower areas, *B. fusca* is predominant in the cooler and higher altitudes areas while *S. calamistis* is found in low densities in all ecologies in Kenya (Ong'amo et al., 2006).

Lepidopteran maize stem borers are serious pests in sub-Saharan Africa region because besides the reduced grain cereal yields, they cause direct losses through loss of photosynthetic leaf area, results in dead hearts which leads to lodging from damaged stems. Plants also suffer from increased ear rots and are predisposed to infections by *Aspergillus flavus* and contamination with mycotoxins (Kfir et al., 2002; Mugo et al., 2012; Muturi et al., 2012). The lepidopteran stem borers, therefore, poses major threats to sustained food sufficiency in sub-Saharan Africa region causing annual yield losses of approximately 15%, and particularly in Kenya where they cause losses estimated at 13.5% (De Groote, 2002). The recommended control methods which include cultural, chemical and biological have not been successful. The most recently recommended control method has been by use of *Bt* (*Bacillus thuringiensis*) gene, however, its use has not been authorised in Kenya and in majority of the sub-Saharan African countries. The *Bt* control solution further remains elusive because recent studies have reported reduced efficacy of *Bt* transgenes as some of the important pests have already developed resistance since its registration in 1996 (Campagne et al., 2013; Jiménez-Galindo et al., 2017). Natural levels of resistance in elite maize varieties remain insufficient to manage the stem borer pest and detection of resistance QTL could enhance breeding for this trait through marker-assisted breeding or genomic selection (Samayoa et al., 2015a). Host plant resistance could be the most economically feasible and ecologically sound method as it is technically and socially acceptable.

The stem borer resistance is quantitatively inherited and progress in breeding for resistance through conventional methods has been slow (Jampatong et al., 2002). Stem borer resistance using conventional breeding methods has been elusive due to limited genetic variation, the difficulty in maintaining a quantitative trait, and having to deal with two organisms; pests and hosts (Mugo et al., 2002). The trait is controlled by many genes of small effects, thus, there has not been any immune inbred lines developed for its control this far. International Maize and Wheat Improvement Center (CIMMYT) has, however, endeavoured to continue developing inbred lines with high resistance levels and commits much resource in maintaining and improving them. Marker assisted selection for this trait might fast track the breeding process for the many regions in sub-Saharan Africa region where maize stem borers remain a threat to food security.

Mapping of quantitative trait loci (QTL) associated with stem borer resistance would be an important step towards improving efficiency in breeding using marker assisted breeding (MAB). To date, there are several molecular markers available and coupled with the completion of sequencing of the sorghum genome (Bedell et al., 2005) provides opportunities to exploit advances in genomics and genetics for resistance breeding. Such markers especially when tightly linked to resistance loci can support the introgression and selection of associated traits in early generations of breeding, thus minimizing the need for extensive and expensive phenotypic analysis (Drinic et al., 2004). Quantitative trait loci (QTL) for insect resistance in some temperate and tropical maize germplasm against various maize stem-borer species have been detected and documented (Bohn et al., 2000; Samayoa et al., 2015b; Jiménez-Galindo et al., 2017). Such results lead to the conclusion that QTL too can be found for resistance to tropical stem borers including *C. partellus* and *B. fusca* and could underpin MAB in the future. It should also be noted that marker-assisted breeding is an expanding breeding frontier to improve the efficiency of plant breeding through the transfer of specific genomic regions of interest and accelerating the recovery of the elite parent background (Robyn, 2008).

Several methods for QTL mapping have been used and include simple interval mapping, composite interval mapping (fairly similar to multiple QTL mapping) and association mapping (Toure et al., 2000). Both simple interval mapping and composite interval mapping are mainly based on maximum likelihood regression and calculate the most likely position of a QTL within a certain interval between two flanking markers. However, though composite mapping is quite similar to simple interval mapping it possesses improved power because it includes additional genetic predictors, called 'cofactors' that represent QTL elsewhere in the genome and which absorb background genetic noise (Van Eeuwijk et al., 2010). Multiple QTL mapping (MQM) method was used in this study because theoretically, it reduces the error

Table 1. Location and description of six test sites where the testcrosses were evaluated during the March to September, 2011 rainy season.

Site name	Longitude	Latitude	Max. (°C)	Min (°C)	Rainfall (mm)	Altitude (masl)	Soils
KALRO Kiboko	37.75'E	2.15'S	35.1	14.3	530	950	Sandy clays
KALRO Kakamega	34.45'SE	0.16'N	28.6	12.8	1915	1585	Sandy loam
KALRO Mtwapa	39.219'E	4.347'S	29.0	12.8	965	30	Sandy
KALRO Embu	37.412'E	0.449'S	25.0	14.1	1200	1510	Clay loam
Kirinyaga University (KYU)	37.19'E	0.34'S	24.0	18.0	1500	1282	Clay loam
Bukura	34.36'E	0.15'N	22.0	20.0	1800	1397	Sandy loam

variance and increases the power for detecting QTL. Multiple QTL mapping (MQM) is a mapping method that has advantages above other QTL mapping methods as it reduces linkage by considering cofactors to obtain a higher power when mapping QTLs. It applies a backward model selection procedure using an analysis of deviance approach. The use of co-factors and employing a backward model selection can help identify previously unknown locations underlying complex traits (Scott et al., 1966; Arends et al., 2010).

While association mapping (linkage disequilibrium mapping) is a recent and more reliable method of locating putative QTL, the method does not deal with a fixed population like interval and multiple QTL mapping but is based on a random and larger population (Yan et al., 2011). Because of the fixed nature of the 203 $F_{2:3}$ populations used in this study, multiple QTL mapping was applied for locating putative QTL. The objective of this study was to map the QTL associated with resistance to *C. Partellus* and *B. fusca* stem borer species in a tropical maize population using stem tunnelling, number of stem borer exit holes and leaf damage score as putative stem borer-resistance traits.

MATERIALS AND METHODS

Field trials for phenotypic data

The $F_{2:3}$ mapping population was developed from the cross between CIMMYT's highly susceptible inbred line CML442 and multiple borer resistant (MBR) inbred line CKSBL10026. These two parents, both developed by CIMMYT were genetically divergent and had great differences for the resistance traits of interest (leaf damage score, cumulative stem tunnel length and number of stem borer exit holes). The F_2 and F_3 progenies were developed by self pollinating previous F_1 and F_2 materials, respectively. Concurrently, three male rows of single cross tester CML395 x CML444 were sown preceding the female $F_{2:3}$ rows. These families were used for the purpose of harvesting leaves for molecular analysis and were also crossed with the single cross tester for seed increase to enable multi locational phenotyping. Leaf samples for molecular analysis were collected from the $F_{2:3}$ generation. Tender leaves from 15 representative plants were picked at seedling stage and transferred to Biosciences east and central Africa (BecA) laboratory in Nairobi and preserved at -80°C. The testcross ears were harvested and a population of 203 selected based on amount of seeds achieved after the hand pollination. These ears were shelled for the purpose of multi-environmental phenotyping.

In March 2011, the 203 $F_{2:3}$ testcrosses were planted for phenotyping across six environments across Kenya that included Kenya Agricultural Livestock Research Organization (KALRO) Kiboko, KALRO Mtwapa, Kirinyaga University, KALRO Kakamega, Bukura and KALRO Embu sites (Table 1). The α- lattice design replicated three times was used in a 2 × 5 m rows plot spaced at 75 cm between rows and 25 cm between plants. *B. fusca* stem borer larvae were used for infestation at Kakamega, Bukura and Embu sites, while *C. partellus* larvae were used for Mtwapa, Kiboko and Kirinyaga University sites. Ten plants in each plot were each artificially infested with five stem borer neonates three weeks after planting. The remaining plants were concurrently treated with an insecticide (Bulldock® 25 EC = 25 g/l Beta-Cyfluthrin - AI) to act as a control. The trials were grown under rain-fed conditions but supplemental irrigation was applied as needed. Fertilizers were applied at the rate of 60 kg/ha N and 102 kg/ha P_2O_5 at planting. The crop was top-dressed at the rate of 48 kg N/ha 30 days after planting. Planting, weeding, harvesting and shelling operations were performed manually.

Data collection

Data was taken on leaf-damage visual-rating score two weeks after infestation on a scale of 1 to 9 on an individual plant basis, according to Tefera et al. (2011), where 1 = no visible leaf damage and 9 = plants dying as a result of leaf damage. At harvest, the numbers of stem exit holes were counted and the cumulative tunnel length (cm) was measured after splitting the maize stems. Grain yield (t/ha) was computed from shelled grain weight and standardized to 12.5% moisture content.

Phenotypic data analysis

Analysis of variance was performed using the PROC GLM procedure SAS package (2007) and the means compared using Fishers protected least significant difference test (LSD) at *"P<0.05"*. Calculation of heritability for both individual and combined sites was done using PROC mixed method of SAS 9 (BLUPS). Due to the zero heritability observed from the Mtwapa site, the site was dropped from combined analysis. A selection index based on leaf damage score, number of stem borer exit holes and cumulative tunnel length was computed by summing up the ratios between values and the overall mean and dividing by the number of damage parameters evaluated. Germplasm with selection indices values less than 0.8 were regarded as highly resistant, 0.8 to 1.0 as moderately resistant, 1.0 to 1.2 as moderately susceptible and above 1.2 as highly susceptible as described in Tefera et al. (2011).

DNA extraction and analysis

Leaf samples from 15 representative three week old seedlings for

Table 2. Heritability for the putative stem borer resistance traits generated through BLUPS (Best linear unbiased predictors).

Individual sites	Heritability		
	Leaf damage score	Exit holes (#)	Tunnel length (cm)
KALRO Kiboko	0.34	0.70	0.84
Kirinyaga University (KYU)	0.69	0.88	0.90
KALRO Kakamega	0.62	0.12	0.11
Bukura	0.93	0.39	0.37
KALRO Embu	0.01	0.23	0.85
Combined *Chilo partellus* sites (Mtwapa, Kiboko, KYU)	0.13	0.00	0.00
Combined *Busseola fusca* sites (Kakamega, Bukura, Embu)	0.02	0.11	0.09

each of the 203 $F_{2:3}$ families were collected in November 2010. DNA was extracted from the lyophilized leaf tissue from 15 $F_{2:3}$ plants of each family in August 2011. DNA extraction was done using the 96-well format high throughput protocol (Mace et al., 2003).

DNA quantity and quality check

After DNA isolation, quality and quantity checks were done using agarose gel electrophoresis and Nanodrop™ (ND-1000) quantification, respectively. The DNA was subjected to electrophoresis using 0.8% agarose gel containing 0.3 µg/mL GelRed (Biotium Inc., USA) at 100V for 45 min in 1× TAE running buffer after which the integrity and intensity of the bands were used to indicate quality and quantity of the DNA. Samples with smeared bands were re-extracted and subjected to electrophoresis once more to confirm integrity. After DNA electrophoresis, the samples were quantified using Nanodrop™ spectrophotometer. Absorbance ratios A_{260}/A_{280} ranging from 1.7 to 2.0 was considered pure with no protein contamination, while A_{260}/A_{230} ratios above 1.5 were considered to be free of salt contaminants. The isolated DNA was normalized to 50 ng/µL using 0.1X TE (10 mM Tris-HCl, pH 7.5 and 0.1 mM EDTA, pH 8.0), and 50 µL of the normalized DNA was shipped to KBiosciences (present LGC genomics) for genotyping. KASPar SNP Genotyping System (allele-specific PCR amplification of target sequences and endpoint fluorescence genotyping) was used for the SNP analyses, and the generated data were used in subsequent analysis.

Single nucleotide polymorphisms (SNPs) marker analysis

One thousand two hundred and thirty (1230) SNPs were initially screened for polymorphism between the parental lines, the F_1s and F_2s. Two hundred and seventy nine (279) out of 1230 SNPs (22.7%) were heterozygote in one or both parents, that is, nine (9) were heterozygote in parent CML442, 265 (21.5%) were heterozygous in the multiple borer resistant parent, and five (5) were heterozygote in both parents. One hundred and ninety-two (192) SNPs were homozygous and polymorphic, and 98.5% of these (184) were true to type for F_1 and F_2. Out of the 184 SNPs, 152 polymorphic SNPs (Appendix 1) were used to genotype the $F_{2:3}$ plants of the 203 individuals, because the chi-square (χ^2) test of fit revealed several markers that had high significance deviations from the 1:2:1 ratio expected for an $F_{2:3}$ populations (*"P<0.001"*), such markers were, therefore, excluded from the linkage map which reduced the markers to 152 SNPs. The linkage map was constructed with the 152 SNP markers using JoinMap 4 software package (Van Ooijen, 2006). Information on the SNPs used is available on maize panzea database website (http://www.panzea.org/database). Segregation at each marker locus was analyzed using chi-square (χ^2) goodness of fit test for the expected Mendelian segregation ratio of an F_2 population. The linkage map was developed using Kosambi's mapping function. A $\log_{10}$ of the likelihood odds ratio (LOD) value of 6.0 was used to construct linkage maps. QTL detection (mapping) was performed using MapQTL 6 (Van Ooijen, 2009). Interval mapping and multiple QTL mapping (similar to composite interval mapping) were used for QTL detection. Automatic cofactors selection function was used to set cofactors for multiple QTL mapping (MQM), a process that allowed markers used as cofactors to absorb the effects of nearby QTL and increases power and precision of QTL analyses. For declaration of linkage, a threshold LOD score of 3.0 and a maximum recombination frequency of 0.50 were used. Series of 1000 permutations were performed to determine experiment wise significance levels at "*P < 0.05*" of LOD 3.0 for both insect species. Interval mapping with LOD score of above 2.5 were assumed to be highly indicative of QTL. Gene action for each QTL was calculated using the dominance ratio using absolute additive and dominance values as described in Stuber et al. (1987). Values of 0 to 0.20 were interpreted for additive gene action, 0.21 to 0.80 as partial dominance, 0.81 to 1.20 as dominance and $\geq$1.20 as over dominance. The source of resistant allele was detected by the +/- of the additive value with reference to the resistant parent CKSBL10026 where negative values showed alleles came from the resistant parent CKSBL10026, and positive additive values showed resistance came from the sensitive parent CML442 as described in Jampatong et al. (2002).

RESULTS

Phenotypic data

In the *C. partellus* infested sites (Kirinyaga University, Mtwapa and Kiboko), only progeny evaluated at Kiboko showed significant differences for number of exit holes and tunnel length. In *B. fusca* infested sites, only progeny evaluated at Bukura showed significant difference for leaf damage. Heritability for resistance traits based on combined sites analysis was low for both stem borer species but high when estimated for evaluations at individual sites except at Mtwapa (Table 2). The selection index computed for all sites and both borer species identified 44 individuals that were highly resistant, 69 moderately resistant, 58 moderately susceptible and 32 highly susceptible with normal distribution frequency (Figure 1). The selection index based on individual stem

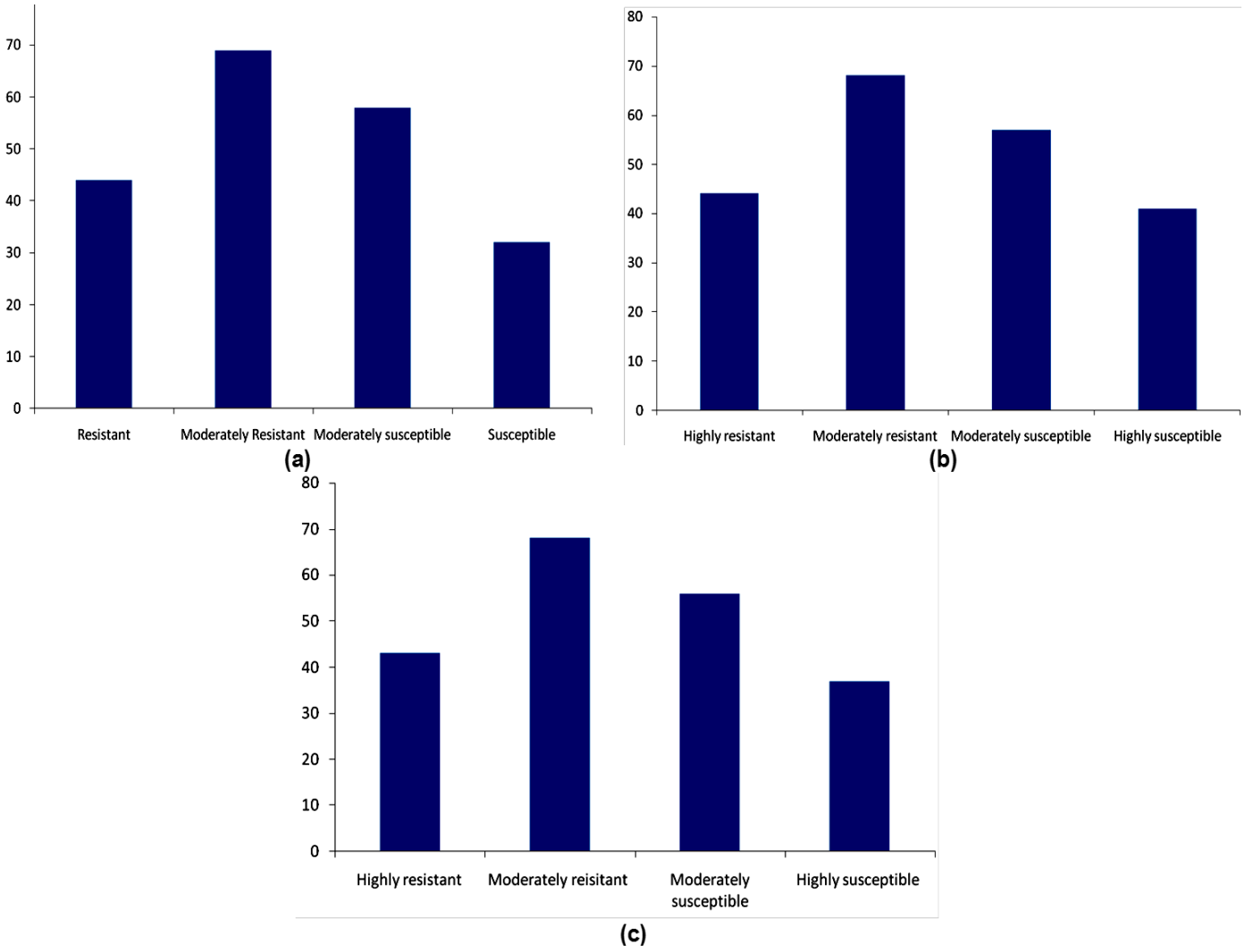

Figure 1. The distribution of genotypes according to resistance categories of the 203 $F_{2:3}$ individuals. (a) Resistance frequency of the 203 $F_{2:3}$ families from combined 6 sites against *C. partellus* and *B. fusca; (*b) Resistance frequency distribution of the 203 $F_{2:3}$ families from combined sites analysis against *C. partellus* species; (c) Resistance frequency distribution of the 203 $F_{2:3}$ families from combined sites analysis against *B. fusca* species. Y-axis represents the actual number of genotypes per category, and the X-axis shows the genotype category names.

borer species such as categorized B. fusca species as 43 progeny as highly resistant, 68 as moderately resistant, 56 as moderately susceptible and 37 as highly susceptible. In the *C. partellus* infested sites, 44 progeny were highly resistant, 68 moderately resistant, 57 moderately susceptible and 41 highly susceptible. Forty-four of the progenies were, therefore, highly resistant to both stem borer species across all locations.

Mapping of the quantitative trait loci

The genetic map was constructed with 152 SNP markers that spanned 1248.01 cM on 10 chromosomes of maize with an average interval length of 8.21 cM. Several QTL for resistance were detected on chromosomes 1, 2, 3, 4, 5, 6, 7 and 9 based on individual sites and different species (Figure 2). Quantitative trait loci detection varied among sites and further, more QTL were detected for *B. fusca* than for the *C. partellus*. In *B. fusca* combined sites analysis, one QTL for resistance to stem tunnelling was detected on chromosome 4 (LOD 2.86) at position 76.33 cM and accounted for 6.2% of phenotypic variation. In the *C. partellus* combined sites, two QTL for stem tunnelling on chromosome 4 (LOD 2.81) and number of stem exit holes on chromosome 5 (LOD 2.53) were detected and accounted for 6.2 and 5.6% of the phenotypic variation, respectively (Table 3).

QTL for resistance to leaf damage

Two (2) QTL affecting leaf damage feeding score were

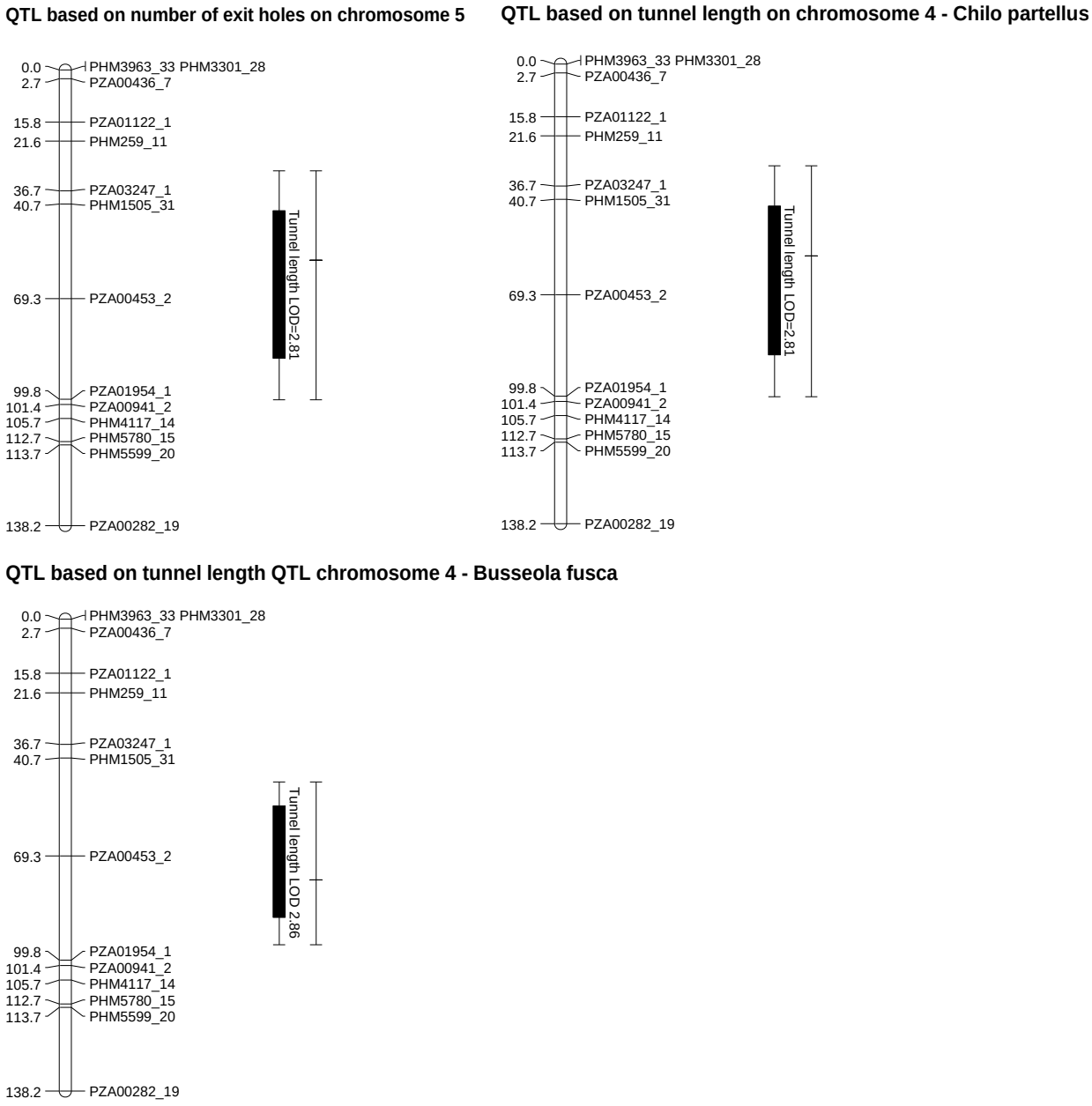

Figure 2. Linkage maps and QTL locations from specific stem borer species (*C. partellus* and *B. fusca*) analysis of the 152 SNPs on leaf damage, number borer exit holes and tunnel length. The line to the left of each QTL bar indicates the QTL peak.

detected on chromosome 2 for Embu site (LOD 3.37) and one indicative QTL on chromosome 1 for Kakamega site (LOD 2.68). The most significant was the QTL detected on the Embu site which explained 6.6% of the phenotypic variation. Gene action was due to over dominance for both QTL.

QTL for resistance to number of exit holes

QTL mapped for *C. partellus* based on combined site analysis revealed 1 QTL (LOD 2.53) for number of exit holes on chromosome 4 but none for *B. fusca*. Conversely, three QTL for resistance to stem exit holes were detected in the individual sites (Kakamega, Kirinyaga University and Bukura sites). Several QTL were detected for progenies evaluated at the following sites; 1 QTL on chromosome 4 at the Kirinyaga University site (LOD 3.73) for *C. partellus* species, 1 on chromosome 9 at Bukura site (LOD 2.97) and a minor QTL (LOD 2.56) on chromosome 1 at Kakamega site for *B. fusca* stem borer species. The most important was the QTL detected

Table 3. Locations and QTL effects for *C. partellus* and *B. fusca* stem borer resistance mapped in $F_{2:3}$ families from the cross between sensitive CML442 and CKSBL10026 multiple borer resistant inbred line parents.

Evaluation sites	Trait	LOD	Chr No.	Locus	Position in cM	% variance explained	Gene effect		Gene action
							Additive	Dominance	
Embu	Leaf damage	3.4	2	PZA02890_4	106.9	6.6	-0.09	0.13	OD
	Tunnel length	2.6	7	PZA00795_1	98.01	5.8	-0.08	0.8	OD
Kakamega	Leaf damage	2.7	1	PHM14614_2	60.9	5.9	0.1	-0.11	OD
	Exit holes	2.6	6	PZA00571_1	39.02	5.5	-0.31	-0.12	PD
	Tunnel length	3	1	PZA03301_2	92.97	6.5	-0.15	-0.2	OD
Kirinyaga University (KYU)	Exit holes	3.7	4	PZA00453_2	69.33	8.1	-0.49	-0.09	A
	Tunnel length	3.2	6	PZA02478_7	57.43	7.1	-0.81	-1.17	OD
Bukura	Exit holes	3.2	9	PZA00152_1	55.41	6.5	-0.17	-0.07	PD
	Tunnel length	3.3	6	PZA00152_2	55.41	6.7	-0.41	-0.2	PD
Kiboko	Tunnel length	2.7	3	PZA03391_1	108.93	5.9	-0.24	-0.84	OD
Combined *C. partellus*	Exit holes	2.5	5	PZA01284_6-PHM13942_7	64.669	5.6	0.126	-0.668	OD
	Tunnel length	2.8	4	PHM1505_31-PZA00453_2	57.741	6.2	0.733	-0.104	PD
Combined *B. fusca*	Tunnel length	2.9	4	PZA00453_2-PZA01954_1	76.329	6.2	-0.0335	-0.837	OD

Chr, Chromosome; LOD, Log_{10} of likelihood odds ratio; OD, over dominance, PD; partial dominance, A; additive gene action.

for *C. partellus* from Kirinyaga University which explained 8% of the phenotypic variation. The QTL detected for *B. fusca* at Bukura site explained 6.5% of the total phenotypic variation while for Kakamega site; the QTL explained 5.5% variation. The gene action for both Bukura and Kakamega sites were due to partial dominance while it was additive gene action for QTL detected for Kirinyaga University site (Table 3).

QTL for resistance to stem tunnelling

Combined sites analysis for both stem borer species revealed stem tunnelling QTL on chromosome 4 (LOD 2.81 for *C. partellus* sites and LOD 2.86 for *B. fusca* sites). Five QTL for reduced tunnelling were detected on different chromosomes on the individual sites for the two stem borer species. The strongest QTL for *C. partellus* stem tunnelling resistance was detected at Kirinyaga University site on chromosome 6 (LOD 3.24), while that for *B. fusca* stem tunnelling resistance was similarly detected for Bukura site on chromosome 6 (LOD 3.33), they explained 7.1 and 6.7% of the phenotypic variation, respectively. Suggestive QTL for resistance to stem tunnelling to *B. fusca* were detected at both Kakamega (LOD 2.99) and Embu (LOD 2.61) sites. A similar indicative QTL for resistance to stem tunnelling against *C. partellus* was detected at Kiboko (LOD 2.67). Stem tunnelling QTL was conditioned by over dominance gene action except for the Bukura QTL which was due to partial dominance.

DISCUSSION

Phenotypic data

The extremely low heritability in the combined sites analysis found in this study was a probable indicator of significant genotype by environmental interactions. In a recent similar study, Jiménez-Galindo et al. (2017) reported that resistance traits are associated with high experimental error because they are affected by the plant genotype,

the pest pressure and the environment and, therefore, are difficult to measure. All these factors lead to insect resistance traits showing low to moderate heritability values. The phenotypic data did not reveal distinct differences in resistance levels in the different sites except at Kiboko and Bukura sites. The high heterozygosity revealed in the parents after screening for polymorphism could have compounded the phenotypic differentiation between resistance and susceptible progenies in the field. This phenomenon may have caused the low levels of trait significance for resistance traits in both individual and combined sites. High and significant differences were, however, recorded for the Kiboko site in stem borer tunnel length and exit holes number, and leaf damage at Bukura site. The selection index computed from the three resistance traits leaf damage, number of borer exit holes and cumulative tunnel length in the combined analysis revealed several individuals that were resistant to *C. partellus* or *B. fusca,* or/and both. Forty four (44) individuals were resistant to both borer species in all sites, a clear confirmation that the resistant parent carried genes for multi-borer resistance. These results agree with the findings of Mwololo et al. (2015) and Odinga et al. (2016) who reported multiple resistances in some tropical maize germplasm against both *C. partellus* and *B. fusca* maize stem borer species. The phenotypic means distribution for resistance traits exhibited a normal distribution curve for specific species sites, and combined sites analyses (Figure 1). This was in agreement with Jampatong et al. (2002) who reported similar phenotypic means distribution for European corn borer resistance mapping study. There was a high correlation between the number of stem borer exit holes and stem tunnelling in the combined sites analysis which was a strong indication of the two parameters reliability and consistence as putative measures of resistance. These findings suggest that these parameters were neither dependent on the environments nor the stem borer species.

Quantitative trait loci for resistance to stem borers

Combined mapping of QTL based on data across sites for both species mapped resistance loci to chromosome 4 for stem tunnelling at position 57.74 cM (LOD 2.81) for *C. partellus* and at position 76.33 cM (LOD 2.86). One QTL for number of exit holes (LOD 2.53) was detected on chromosome 5 for *C. partellus* at position 64.67 cM. The close proximity of these stem tunnelling QTL within 18 cM on chromosome 4 for the both stem borer species suggested that there could be a gene with significant effects on reduced stem tunnelling between positions 57.74 and 76.33 cM. In other studies of a related lepidopteran pest (the European corn borer), QTL for resistance traits occurred in clusters (Papst et al., 2005). It is thus possible that in the case of resistance to stem borer in tropical maize, similar genome setup may occur as found in this study. Quantitative trait loci for resistance to stem borers mapped based on data from individual sites were mostly inconsistent, with only two sites (Kirinyaga University and Bukura) having consistently revealed QTL on chromosome 6. These inconsistencies in QTL detection may have been due to low levels of segregation in the mapping population, or it could underscore the enormous contribution and interaction of the environmental effects on QTL detection. Several QTL may, therefore, have been undetected in this study due to the environmental effects. Similar results have been reported in other studies on the European corn borer due to environmental effects (Jampatong et al., 2002; Krakowsky et al., 2004). The phenotypic variances associated with the QTL reported in this study were fairly low (mostly slightly below 10%). This study was in agreement with other QTL mapping studies in maize that reported low phenotypic variances on both the European corn borer, and storage insect pests (Jampatong et al., 2002; Garcia-Lara et al., 2009; Samayoa et al., 2015b; Jiménez-Galindo et al., 2017). Small phenotypic variation values may suggest that the QTL have only small effects, or have larger effects but were only more loosely linked to the marker locus (Edwards et al., 1987; Bohn et al., 2000).

The detected QTL in this study were conditioned by over dominance, partial dominance and additive gene actions. In 12 of the 13 QTL detected, resistance was conditioned by over-dominance and partial dominance. Partial dominance was found on three (3) QTLs for number of exit holes and stem tunnelling whilst additive gene action accounted for 1 QTL for the number of exit holes. In maize, resistance to the European corn borer is conditioned in a similar manner, albeit with additive gene action accounting for the majority of the QTL than dominance and over dominance gene actions (Guthrie and Russell, 1989; Bohn et al., 2000; Krakowsky et al., 2004; Jampatong et al., 2002). Scott et al. (1966) showed that resistance to the European corn borer, a lepidopteran pest just like *C. partellus* and *B. fusca* was conditioned by a relatively large number of genes with small effects on chromosomes 1, 2, 4, 6 and 8. The caution is that some QTL may not have been detected and, or, were dissimilar to those reported for related stem borers species due to the low heritability of the putative traits, and differences in trait characterization (Khairallah et al., 1998; Jiménez-Galindo et al., 2017). In a similar study, Samayoa et al. (2015b) attributed such discrepancies to QTL by environment interaction effects and stressed the importance of making phenotypic evaluations in environments similar to those for which breeding materials are intended to be used.

Overall these results show the presence of QTL for maize stem borer resistance in the tropical maize population studied and thus could provide an opportunity to pyramid them into elite material as has been done for

the European corn borer (Jampatong et al., 2002). Majority of the LOD scores were below 3.0 (at *"P<0.05"*), and that was most likely due to the low heritability of the trait under study, and phenotype differences under the different environments. The probability of detecting strong QTL with small sample sizes should be comparatively low unless the QTL explains a substantial proportion of the genetic variance. Melchinger et al. (1998) also reported that with a large number of minor QTLs influencing a quantitative trait such as insect resistance, the power of QTL detection and number of common QTLs should be smaller than for a trait governed by a small number of major QTL. The low heritability for stem borer resistance which was indicative of their polygenic nature should not be considered an impediment to maize improvement breeding activities in the tropics or elsewhere (Stuber et al., 1987; Bohn et al., 2000; Garcia-Lara et al., 2009).

Conclusions

Quantitative trait loci for the three putative resistance traits were detected in the tropical maize population studied. Relative to other maize stem borer QTL mapping studies, fewer QTL were detected in this study. Among the three traits, QTL for stem tunnelling were the strongest and were the most detected in both individual and combined specific borer species environments. The variances explained by QTL-marker associations were, however, low, indicative of many QTL with small variances that could have escaped detection. Individual sites analysis revealed stronger QTL and it was noted that more QTL were detected against *B. fusca* than *C. partellus*. The low reproducibility of QTL across environments for both stem borer species underscores the need for finer mapping and need for larger populations in succeeding mapping activities in the tropics.

CONFLICT OF INTERESTS

The authors declare that there are no conflicts of interests.

ACKNOWLEDGEMENTS

The Regional Universities Forum for Capacity Building in Agriculture (RUFORUM) and the Syngenta Foundation for Sustainable Agriculture through the Development of Resistant Maize to Stem Borer and Storage Insect Pests for Eastern and Southern Africa Project (IRMA III) are appreciated for co-funding this research. Joel Mbithi and Patrick Gichobi, CIMMYT Kiboko field staff; David Karuri (KALRO-Embu), Grace Ambajo (KALRO-Mtwapa) and Gabriel Ambani (KALRO-Kakamega) are appreciated for their contributions to the success of the multi-location field evaluations. This was part of the first author's PhD dissertation research study.

REFERENCES

Arends D, Prins P, Jansen RC, Broman KW, Barrett J (Ed.) (2010). R/qtl: high-throughput multiple QTL mapping. Bioinformatics 26:2990-2992.

Bedell JA, Budiman MA, Nunberg A, Citek RW, Robbins, D (2005). Sorghum genome sequencing by methylation filtration. PLoS Biol. 3(1):e13.

Bohn M, Schulz B, Kreps R, Klein D, Melchinger AE (2000). QTL mapping for resistance against the European corn borer (*Ostrinia nubilalis* H.) in early maturing European dent germplasm. Theor. Appl. Genet. 101:907-917.

Calatayud PA, Le Ru BP, van den Berg J, Schulthess F (2014). Ecology of the African Maize Stalk Borer, Busseola fusca (Lepidoptera: Noctuidae) with Special Reference to Insect-Plant Interactions. Insects 5:539-563.

Campagne P, Kruger M, Pasquet R, Le Ru B, Van den Berg J (2013). Dominant Inheritance of Field-Evolved Resistance to *Bt* Corn in *Busseola fusca*. PLoS ONE 8(7):e69675.

De Groote H (2002). Maize yield losses from stem borers in Kenya. Insect Sci. Appl. 22:89-96.

Drinic SM, Micic DI, Eric I, Andelkovic V, Jelova D, Konstantinov K (2004). Biotechnology in breeding. Genetika 36:93-109.

Edwards MD, Stuber CW, Wendel JF (1987). Molecular-Marker-Facilitated Investigations of Quantitative-Trait Loci in Maize. I. Numbers, Genomic Distribution and Types of Gene Action. Genetics 116:113-125.

Garcia-Lara S, Khairallah MM, Vargas M, Bergvinson DJ (2009). Mapping of QTL Associated with Maize Weevil Resistance in Tropical Maize. Crop Sci. 49:139-149.

Guthrie WD, Russell WA (1989). Breeding methodologies and genetic basis of resistance in maize to the European corn borer. In. CIMMYT, ed. Towards Insect Resistant Maize for the Third World. Proceedings of the International Symposium on Methodologies for Developing Host Plant Resistance to Maize Insects. Mexico, D.F. pp. 192-202.

Jampatong C, McMullen MD, Barry BD, Darrah LL, Byrne PF, Kross H (2002). Quantitative Trait Loci for First- and Second-Generation European corn borer Resistance Derived from the Maize Inbred Mo47. Crop Sci. 42:584-593.

Jiménez-Galindo JC, Ordás B, Butrón A, Samayoa FL, Malvar RA (2017). QTL Mapping for Yield and Resistance against Mediterranean Corn Borer in Maize. Front. Plant Sci. 8:698.

Kfir R, Overholt WA, Khan ZR, Polaszek A (2002). Biology and management of economically important lepidopteran cereal stem borers in Africa. Annu. Rev. Entomol. 47:701-731.

Khairallah MM, Bohn M, Jiang C, Deutsch JA, Jewell DC, Mihm JA, Melchinger AE, Gonzalez-de-leon, D, Hoisington DA (1998). Molecular mapping of QTL for south-western corn borer resistance, plant height and flowering in tropical maize. Plant Breed. 117:309-318.

Krakowsky M, Lee M, Woodman-Clikeman WL, Long MJ, Sharopova N (2004). QTL Mapping of Resistance to Stalk Tunnelling by the European Corn Borer in RILs of Maize Population B73 Ã— De81. Crop Sci. 44:274-282.

Mace ES, Buhariwalla HK, Crouch JH (2003). A high-throughput DNA extraction protocol for tropical molecular breeding programs. Plant Mol. Biol. Rep. 21:459-460.

Mailafiya DM, Le Ru BP, Kairu EW, Stéphane D, Paul-André C (2011). Parasitism of lepidopterous stem borers in cultivated and natural habitats. J. Insect Sci. 11:15-25.

Melchinger H, Friedrich U, Chris CS (1998). Quantitative Trait Locus (QTL) Mapping Using Different Testers and Independent Population Samples in Maize Reveals Low Power of QTL Detection and Large Bias in Estimates of QTL Effects. Genetics 149:383-403.

Mihm JA (ed.) (1997). Insect Resistant Maize: Recent Advances and Utilization; Proceedings of an International Symposium held at the

International Maize and Wheat Improvement Center (CIMMYT) 27 November-3 December, 1994. Mexico, D.F.: CIMMYT.
Mugo S, Songa J, DeGroote H, Hoisington D (2002). Insect Resistant Maize for Africa (IRMA) Project: An overview. CIMMYT, Washington DC.
Mugo S, Tefera T, Beyene Y (2012). Stem Borer Pest Resistant Maize: An Update from Africa. Presented to the SI 4 Stress tolerant maize for the poorest (Tues 17th Jan., 2012, Session M1 – Group 1) During the Global Launch of the MAIZE and WHEAT CGIAR Research Programs, Mexico City, 16-20 Jan 2012.
Muturi PW, Rubaihayo P, Mgonja M, Kyamanywa S, Sharma HC, Hash CT (2012). Novel source of sorghum tolerance to the African stem borer, *Busseola fusca*. Afr. J. Plant Sci. 6:295-302.
Mwololo JK, Munyiri SW, Semagn K, Mugo S, Okori P (2015). Genetic Diversity Analysis in Tropical Maize Germplasm for Stem Borer and Storage Pest Resistance using Molecular Markers and Phenotypic traits. Mol. Plant Breed. 6:1-22.
Odinga R, Karua JC, Awori TG, Nicholas CK (2016). Assessment of the response of tropical maize inbred lines in resistance to *B. fusca* and *C. partellus in* Eastern Africa. Int. J. Plant Breed. Genet. 3:189-199.
Ong'amo GO, Le Ru BP, Dupas S, Moyal P, Calatayud PA, Silvain JF (2006). Distribution, pest status and agro-climatic preferences of lepidopteran stem borers of maize in Kenya. Ann. Soc. Entomol. Fr. 42:171-177.
Papst C, Bohn M, Utz HF, Melchinger AE, Klein D, Eder J (2005). Evaluation of resistance factors against European corn borer (*Ostrinia nubilalis* HBn.) in central European dent material. Proceedings of the 54th Annual Meeting of the growers and the seed merchants Austria: Hybrid maize breeding and utilization, 25-27 November 2003, Gumpenstein Irdning, Austria.
Robyn S (2008). Prospects for using marker-assisted breeding to improve maize production in Africa. J. Sci. Food Agric. 88:745-755.
Samayoa LF, Malvar RA, McMullen MD, Butrón A (2015b). Identification of QTL for resistance to Mediterranean corn borer in a maize tropical line to improve temperate germplasm. BMC Plant Biol. 15:265.
Samayoa LF, Malvar RA, Olukolu BA, Holland JB, Butrón A (2015a). Genome-wide association study reveals a set of genes associated with resistance to the Mediterranean corn borer (Sesamia nonagrioides L.) in a maize diversity panel. BMC Plant Biol. 15:35.
SAS (2007). Proceedings of the Twenty-Eighth Annual SAS®Users Group International Conference. SAS Institute Inc., Cary, NC, USA.
Scott GE, Dicke FF, Pesho GR (1966). Location of genes conditioning resistance in corn to leaf feeding of the European corn borer. Crop Sci. 6:444-446.
Smale M, Byerlee D, Jayne T (2011). Maize revolutions in sub-Saharan Africa. Policy Research Working Paper 5659. World Bank Development Research Group: Agriculture and Rural Development Team.
Stuber CW, Edwards MD, Wendel JF (1987). Molecular Marker-Facilitated Investigations of Quantitative Trait Loci in Maize. II. Factors Influencing Yield and Its Component Traits. Crop Sci. 27:639-648.
Tefera T, Mugo S, Tende R, Likhayo P (2011). Methods of Screening Maize for Resistance to Stem Borers and Post-harvest Insect Pests. International Maize and Wheat Improvement Centre (CIMMYT). Nairobi. Kenya.
Toure A, Haussmann BIG, Jonesc N, Thomasd H, Oughame H (2000). Application of molecular markers in plant breeding, B. I. G. Haussmann, et al., (eds.) Training manual for a seminar held at IITA, Ibadan, Nigeria from 16-17 August 1999. International Crops Research Institute for the Semi-Arid Tropics (ICRISAT), Patancheru 502 324, Andhra Pradesh, India.
Van Eeuwijk FA, Bink MC, Chenu K, Chapman SC (2010). Detection and use of QTL for complex traits in multiple environments. Curr. Opin. Plant Biol. 13:193-205
Van Ooijen JW (2006). JoinMap ® 4, Software for the calculation of genetic linkage maps in experimental populations. Kyazma B.V., Wageningen, Netherlands.
Van Ooijen JW (2009). MapQTL ® 6 Software for mapping quantitative trait loci in experimental populations of diploid species. Kyazama B.V., Wageningen, Netherlands.
Yan J, Warburton M, Crouch J (2011). Association Mapping for Enhancing Maize (*Zea mays* L.) Genetic Improvement. Crop Sci. 51:433-444.

Appendix 1. List of SNP markers used to generate the genetic maps.

No.	SNP-Chromosome	No.	SNP-Chromosome	No.	SNP-Chromosome	No.	SNP-Chromosome	No.	SNP-Chromosome
1	PHM13942_7Chr5	34	PZA00152_1Chr9	67	PZA03301_2Chr1	99	PZB01403_1Chr1	131	PZA00664_3Chr1
2	PHM4752_17Chr1	35	PZA00245_20Chr1	68	PZA03391_1Chr3	100	csu1171_2Chr1	132	PZA00750_1Chr3
3	PHM5794_13Chr6	36	PZA00255_14Chr5	69	PZA03409_1Chr4	101	PHM10621_29Chr1	133	PZA00795_1Chr7
4	PZA00191_5Chr5	37	PZA00273_5Chr5	70	PZA03461_1Chr6	102	PHM11946_19Chr9	134	PZA00838_2Chr8
5	PZA00424_1Chr7	38	PZA00300_14Chr5	71	PZA03527_1Chr3	103	PHM1218_6Chr9	135	PZA00910_1Chr6
6	PZA00892_5Chr3	39	PZA00418_2Chr7	72	PZA03577_1Chr2	104	PHM14475_7Chr1	136	PZA01122_1Chr4
7	PZA01257_1Chr8	40	PZA00453_2Chr4	73	PZA03605_1Chr10	105	PHM1505_31Chr4	137	PZA01210_2Chr7
8	PZA02117_1Chr1	41	PZA00498_5Chr8	74	PZB00901_3Chr2	106	PHM1511_14Chr2	138	PZA01374_1Chr2
9	PZA03713_1Chr10	42	PZA00706_16Chr8	75	PZB01009_2Chr6	107	PHM15331_16Chr10	139	PZA01462_1Chr6
10	PZD00027_2Chr3	43	PZA00942_2Chr6	76	PZB01062_3Chr1	108	PHM16125_47Chr2	140	PZA01470_1Chr8
11	PHM11114_7Chr8	44	PZA00978_1Chr1	77	PZB01647_1Chr1	109	PHM18513_156Chr10	141	PZA01542_1Chr7
12	PHM12830_14Chr7	45	PZA00986_1Chr7	78	PZD00022_5Chr2	110	PHM1968_22Chr1	142	PZA01570_1Chr5
13	PHM15449_10Chr3	46	PZA01028_2Chr7	79	sh1_12Chr9	111	PHM2518_28Chr4	143	PZA01591_1Chr6
14	PHM1932_51Chr1	47	PZA01241_2Chr10	80	PHM14614_22Chr1	112	PHM2658_129Chr6	144	PZA01642_1Chr10
15	PHM2487_6Chr8	48	PZA01246_1Chr1	81	PHM2691_32Chr7	113	PHM2691_31Chr7	145	PZA01779_1Chr5
16	PHM259_11Chr4	49	PZA01284_6Chr5	82	PHM2919_23Chr3	114	PHM3078_12Chr7	146	PZA01954_1Chr4
17	PHM2714_11Chr8	50	PZA01297_1Chr8	83	PHM3301_28Chr4	115	PHM3334_4Chr2	147	PZA01978_23Chr1
18	PHM2769_43Chr5	51	PZA01438_1Chr5	84	PHM3896_9Chr10	116	PHM4145_18Chr3	148	PZA02040_2Chr5
19	PHM3147_18Chr1	52	PZA01501_1Chr3	85	PHM3963_33Chr4	117	PHM4604_18Chr9	149	PZA02164_16Chr5
20	PHM3334_6Chr2	53	PZA01799_1Chr9	86	PHM4080_15Chr7	118	PHM4780_38Chr2	150	PZA02167_2Chr2
21	PHM3337_23Chr8	54	PZA01933_3Chr7	87	PHM5529_4Chr6	119	PHM4786_9Chr8	151	PZA02385_6Chr4
22	PHM3598_20Chr2	55	PZA02019_1Chr8	88	PHM595_30Chr1	120	PHM499_19Chr2	152	PZA02478_7Chr6
23	PHM3736_11Chr10	56	PZA02247_1Chr6	89	PZA00224_4Chr2	121	PHM5296_6Chr5		
24	PHM4117_14Chr4	57	PZA02383_1Chr5	90	PZA00282_19Chr4	122	PHM5359_10Chr5		
25	PHM4620_24Chr2	58	PZA02423_1Chr3	91	PZA00381_4Chr1	123	PHM537_22Chr10		
26	PHM4997_17Chr1	59	PZA02549_3Chr2	92	PZA00818_1Chr5	124	PHM789_16Chr5		
27	PHM5306_16Chr1	60	PZA02653_12Chr5	93	PZA00860_1Chr9	125	PHM7953_11Chr2		
28	PHM533_46Chr5	61	PZA02698_3Chr1	94	PZA00941_2Chr4	126	PZA00081_18Chr1		
29	PHM5599_20Chr4	62	PZA02769_1Chr5	95	PZA01301_1Chr8	127	PZA00111_10Chr7		
30	PHM565_31Chr5	63	PZA02872_1Chr7	96	PZA01445_1Chr1	128	PZA00256_27Chr7		
31	PHM5780_15Chr4	64	PZA02890_4Chr2	97	PZA02129_1Chr1	129	PZA00436_7Chr4		
32	PHM662_27Chr5	65	PZA02955_3Chr8	98	PZA02186_1Chr1	130	PZA00571_1Chr6		
33	PHM7584_9Chr9	66	PZA03001_15Chr1	99	PZA02328_5Chr6	131	PZA00581_3Chr3		

No., Number.

African Journal of Biotechnology

Related Journals Published by Academic Journals

- *Biotechnology and Molecular Biology Reviews*
- *African Journal of Microbiology Research*
- *African Journal of Biochemistry Research*
- *African Journal of Environmental Science and Technology*
- *African Journal of Food Science*
- *African Journal of Plant Science*
- *Journal of Bioinformatics and Sequence Analysis*
- *International Journal of Biodiversity and Conservation*

academicJournals